Bulletin of the Earthquake
Research Institute
Vol. 46 (1968), pp. 75-123

5. A Model of the Bottom Boundary Layer in Water Waves.

By Kinjiro Kajiura,
Earthquake Research Institute.

(Read Sept. 12, 1967.—Received Nov. 18, 1967.)

Abstract

On the basis of an eddy viscosity assumption compatible with the two-layer model (wall and defect layers) of the turbulent boundary layer, a method of calculating various characteristics of the wave boundary layer, such as the friction coefficient, universal profiles of the stress and velocity in the defect layer have been developed.

Numerical results show that amplitude and phase of the friction coefficient increase with the decrease of the amplitude of the reference velocity and/or the period of wave. The criteria for the smooth-rough and laminar-turbulent transitions are also suggested from the analogy to the case of steady flow.

Most of the experimental data on the friction coefficint and the velocity profile in a wave boundary layer seem to be favorably compared with the prediction derived from the present model.

1. Introduction

The knowledge about bottom friction under waves is required to understand various phenomena related to wave modification and sediment movement in shallow water. Although the case of laminar flow has been clarified to a considerable degree by Iwagaki *et al.* (1967), the structure of the turbulent frictional boundary layer under waves is not well understood, so that the friction law applicable to the oscillatory turbulent flow is quite ambiguous.

Bagnold (1946) was the first to give an empirical formula of the friction coefficient of the quadratic friction law for an oscillatory flow in the presence of artificial ripples. He found that the friction coefficient decreases with the increasing excursion distance; namely with increasing period and/or the amplitude of velocity oscillation. Putnam and Johnson (1949) took Bagnold's formula into account and adopted

0.01 as a reasonable value for the friction coefficient for wind waves and swells in their discussion of the dissipation of wave energy in shallow water. However, the field observations of wave decay in shallow water by Bretchneider (1954) and by Iwagaki and Kakinuma (1965) indicated much larger values than 0.01 for the friction coefficient, and, in particular, the results by the latter showed the tendency of the friction coefficient to decrease with the increase of wave period. On the other hand, laboratory experiments on wave decay over a sandy bottom were presented by Savage (1953), Inman (1962), and Zhukovets (1963). According to Savage (1953), the wave decay depends on the stage of the development of sand ripples compatible to the existing water wave, and the energy dissipation is smaller in the final, stable state compared with the initial, unstable state of sand ripples. This indicates the important difference between the artificial ripples and the natural sand ripples.

In the ordinary method of bottom stress estimation by means of the energy dissipation of waves, the phase difference between the reference velocity and the bottom stress is not explicity taken into account, although the energy dissipation is related to the in-phase components of the bottom stress and the reference velocity. It is well known that, for a laminar case, the bottom stress and the water particle velocity just outside the wave boundary layer have the phase difference of $\pi/4$, and, for the turbulent case, too, the phase difference is expected if the boundary layer is very thin. Indeed, Lukasik and Grosch (1963) found a thin wave boundary layer in their field observation of ocean swell. Since the bottom friction and the phase difference between the bottom stress and the reference velocity are intimately related to the velocity profile near the bottom, it is very important to study the structure of the wave boundary layer. However, this kind of study is very rare, except for the observation in tidal currents, because of the difficulty of observation. In this regard, Jonsson's contribution (1963) is important. According to his experiment on a turbulent wave boundary layer, the velocity profile near the bottom is logarithmic and the phase difference exists between the bottom shear stress and the reference velocity outside the frictional layer. Based on the experimental result, he proposed formulas for the friction coefficient and the boundary layer thickness. Later he (Jonsson, 1967) summarized the empirical knowledge and attempted to delineate the viscous-turbulent and smooth-rough flow regimes in wave boundary layer for short period wave motions. Recently,

Yalin and Russel (1966) also discussed the friction over a rough surface under waves and pointed out the importance of the phase difference between the reference velocity and the bottom stress, by indicating the dependence of the bottom stress on both the reference velocity and the surface slope.

To understand the frictional processes in the turbulent oscillatory flow, a theoretical model was presented by the author (Kajiura, 1964, hereafter referred to as [1]). The basic idea was to consider the average state of turbulence over one wave period and to adopt the assumption of the eddy viscosity analogous to that for the steady turbulent flow. This theory enables us to estimate the thickness of the frictional boundary layer and the velocity profile in an oscillatory flow. Consequently, the frictional coefficient is given as a function of certain non-dimensional parameters constructed from known quantities of wave and bottom conditions.

In the present paper, some modification of the model presented in Paper [1] is attempted by introducing the concept of wall and defect layers, which seems to be adequate for the case of short period waves, in which the thickness of the bottom frictional layer is very thin compared with the total depth of water, and the results are compared with the experimental findings published so far.

2. Elementary considerations on the bottom friction

It may be instructive at first to consider some diagnostic relations derived from the equation of the oscillatory motion in the frictional layer. If we assume that the total thickness δ of the bottom frictional layer is very small compared with the wave length of the potential wave considered, and the non-linear effect is negligible (except turbulence), the equation of oscillatory mean motion in the layer may be considered predominantly horizontal and is given by

$$\frac{\partial}{\partial t}(u-U)=\frac{\partial}{\partial z}\left(\frac{\tau}{\rho}\right), \tag{2-1}$$

where t is time, z is the vertical co-ordinate directed upwards with the origin at the bottom, u is the horizontal velocity, and τ is the horizontal shear stress with ρ the density of water. U is the horizontal velocity near the bottom derived from the potential theory of waves and is given by

$$\frac{\partial U}{\partial t}=-\frac{1}{\rho}\frac{\partial p}{\partial x}, \tag{2-2a}$$

where $\partial p/\partial x$ is the horizontal pressure gradient near the bottom. Since the thickness δ is assumed small compared with the wave length, it is reasonable to put

$$\frac{\partial U}{\partial z}=0, \quad \text{for} \quad 0<z<\delta. \tag{2-2b}$$

The boundary conditions are

$$u=0 \quad \text{at} \quad z=0, \tag{2-3a}$$

$$\tau\to 0 \quad \text{as} \quad z\to\delta. \tag{2-3b}$$

It should be noticed that in this formulation of the problem, the total depth of water H does not play a role in the processes within the frictional layer if $\delta<H$, provided that $\partial p/\partial x$ or U is given at the top of the frictional layer. In the extreme case of a shallow water wave, however, δ may be limited by the depth of water H.

If we formulate the energy equation from (2-1), the energy dissipation E within the bottom frictional layer per unit area per unit time is given by

$$E=-\int_0^\delta u\frac{\partial \tau}{\partial z}dz. \tag{2-4}$$

(2-4) may be transformed to

$$E=-\int_0^\delta U\frac{\partial \tau}{\partial z}dz-\int_0^\delta (u-U)\frac{\partial \tau}{\partial z}dz. \tag{2-5}$$

Partially integrating the first term and substituting (2-1) into the second term of the right hand side of (2-5), we have

$$E=U\tau_B-\frac{\rho}{2}\int_0^\delta \frac{\partial}{\partial t}(u-U)^2dz, \tag{2-6}$$

where τ_B is the bottom stress and the conditions (2-2b), (2-3b) are taken into account. If averaged over one wave period, the second term of the right hand side vanishes because of the periodicity of the motion, and we arrive at

$$<E>=<U\tau_B>, \tag{2-7}$$

where $<>$ denotes the time average over one wave period.

Now, we define the vertical average velocity $\bar{u}$ by

$$\bar{u}=\frac{1}{\delta}\int_0^\delta u dz, \tag{2-8}$$

and write the oscillatory quantities with the angular frequency σ in complex form:

$$U=\hat{U}e^{i\sigma t}, \tag{2-9a}$$

$$\bar{u}=\hat{\bar{u}}e^{i(\sigma t+\varphi)}, \tag{2-9b}$$

$$\tau_B=\hat{\tau}_B e^{i(\sigma t+\theta)}, \tag{2-9c}$$

where $\wedge$ denotes the real amplitude, φ and θ are the phase lead of $\bar{u}$ and τ_B relative to U. The phase lead θ' of τ_B relative to $\bar{u}$ is given by

$$\theta'=\theta-\varphi. \tag{2-10}$$

The integration of (2-1) with respect to z for the whole frictional layer yields

$$\delta\frac{\partial}{\partial t}(U-\bar{u})=\tau_B/\rho \tag{2-11}$$

and the substitution of (2-9a, b, c) into (2-11) gives

$$\hat{\tau}_B/\rho=\hat{U}\sigma\delta(1-2r\cos\varphi+r^2), \tag{2-12}$$

$$r\cos\theta'=\cos\theta, \tag{2-13}$$

where $r=\hat{\bar{u}}/\hat{U}$. It is interesting to notice in (2-13) that the components of the potential velocity U and the mean velocity $\bar{u}$ in phase with the bottom stress τ_B are equal, so that the mean energy dissipation $<E>$ given by (2-7) is written in the form

$$<E>=\begin{cases}\frac{1}{2}\hat{\tau}_B\hat{U}\cos\theta, & \text{(2-14a)}\\ \frac{1}{2}\hat{\tau}_B\hat{\bar{u}}\cos\theta'. & \text{(2-14b)}\end{cases}$$

The two limiting cases, when i) the pressure gradient force is

almost balanced by the frictional force and ii) the pressure gradient force is almost balanced by the inertial force, can be examined easily by means of (2-12) and (2-13). In the first case, which is analogous to a steady channel flow, we may consider $\delta/H\to 1$, $r\to 0$, $\theta'\to 0$, so that $\hat{\tau}_B/\rho\to\hat{U}\sigma H$, $\theta\to\pi/2$. In the second case, which is encountered for relatively short period waves, we may take $\delta/H\to 0$, $r\to 1$, so that $\varphi\to 0$, $\hat{\tau}_B/\rho\to\hat{U}\sigma\delta\times\{(1-r)^2+\varphi^2\}$, and $\tan\theta=(1-r)/\varphi$.

Although δ is a convenient length scale to discuss the structure of the frictional layer, it is advantageous to introduce more definite length scales in analogy with the displacement thickness and the scale of the defect layer commonly used in the steady turbulent flow. Furthermore, it is convenient to define the friction velocity u^* and the friction coefficient C in parallel to the case of steady turbulent flow. Thus, we define the following quantities:
the amplitude of the bottom friction velocity $\hat{u}_B^*$:

$$(\hat{u}_B^*)^2=\hat{\tau}_B/\rho, \tag{2-15}$$

the modified friction velocity u^*:

$$\hat{u}_B^* u^*=\tau/\rho, \tag{2-16}$$

the wave displacement thickness δ^*:

$$\hat{U}\delta^*=\mathrm{Amp.}\int_0^\delta (U-u)dz, \tag{2-17}$$

the scale of the defect layer Δ:

$$\hat{u}_B^*\Delta=\mathrm{Amp.}\int_0^\delta (U-u)dz, \tag{2-18}$$

the wave friction coefficient[1] C:

$$C\hat{U}U=\tau_B/\rho. \tag{2-19}$$

Taking (2-9a, c) into account, (2-19) may be written as

$$C=\hat{C}e^{i\theta}, \tag{2-20}$$

1) In Paper [1], $C^{(1)}$ is defined in terms of $\overline{u}$ in the form

$$\tau_B/\rho=C^{(1)}\tilde{\overline{u}}\,\overline{u}, \qquad \tilde{\overline{u}}=\left(\frac{8}{3\pi}\right)\hat{\overline{u}}. \tag{A}$$

However, for the deep water case, $\overline{u}$ approaches U, so that the friction coefficient becomes identical in both forms, (A) and (2-19), if we replace $\tilde{\overline{u}}$ by $\hat{\overline{u}}$.

and

$$\hat{C}\hat{U}^2=\hat{\tau}_B/\rho. \tag{2-21}$$

Or, by the combination of (2-16) and (2-19),

$$u_B^*/U=\hat{C}^{1/2}e^{i\theta}. \tag{2-22}$$

In terms of the friction coefficient C, the mean energy dissipation $<E>$ given by (2-14a) becomes

$$<E>=(\rho/2)\hat{C}\hat{U}^3\cos\theta. \tag{2-23}$$

In ordinary definition of the drag coefficient C_f $(=2\tau_B/(|U|U))$ without taking the phase difference between the bottom stress and the reference velocity into account, the wave energy dissipation due to bottom stress is given by

$$<E>=\left(\frac{2}{3\pi}\right)\rho C_f\hat{U}^3, \tag{2-24}$$

(*i.g.*, Putnam and Johnson, 1949) and the comparison of (2-23) and (2-24) shows that

$$C_f/2=(3\pi/8)\hat{C}\cos\theta. \tag{2-25}$$

By inspecting (2-1) and (2-9a, c) together with (2-17) and (2-18), it is easily found that

$$\hat{\tau}_B/\rho=\begin{cases}\hat{U}\sigma\delta^* & \text{(2-26a)}\\ \hat{u}_B^*\sigma\Delta & \text{(2-26b)}\end{cases}$$

and making use of the definitions of u_B^* and C, we may write (2-26a, b) in the form:

$$\delta^*=\hat{C}\hat{U}/\sigma=\hat{C}^{1/2}\hat{u}_B^*/\sigma, \tag{2-27a}$$

$$\Delta=\hat{u}_B^*/\sigma=\hat{C}^{1/2}\hat{U}/\sigma. \tag{2-27b}$$

If we remember that $\hat{U}/\sigma$ is the amplitude of the horizontal movement of a water particle near the bottom when the frictional effect is absent, and C is of the order less than unity, the thickness δ^* is found to be very small compared with the wave length of the potential wave under consideration so that the assumption of (2-2b) is justified.

Now, (2-26a) can be transformed to

$$\delta^* \text{ Amp. } [\partial p/\partial x]/\hat{\tau}_B=1, \tag{2-28}$$

because of the condition (2-2a). The left hand side of (2-28) is analogous to the pressure gradient parameter for the case of the steady turbulent boundary layer. For relatively shallow water when δ^* is limited by the total water depth H, (2-28) becomes

$$\hat{\tau}_B=H \text{ Amp. } [\partial p/\partial x], \tag{2-29}$$

which is analogous to the expression for the bottom stress in a steady channel flow. In this case, (2-27a) gives $\hat{C}=(\sigma H)/\hat{U}$ and the phase θ increases up to $\pi/2$ with the increase of $\hat{U}/(\sigma H)$. On the other hand, for the deep water case when $\delta^* \ll H$, the main frictional effect is limited to a small portion of the water column and the frictional processes are more likely similar to the case of the turbulent boundary layer. This type of flow is realized for $\hat{U}/(\sigma H) \ll 1/\hat{C}$. In the present paper, we forcus our attention to the frictional layer of the boundary layer type. For $\hat{U}/(\sigma H) \geqslant 1/(10\hat{C})$, it is better to define the quadratic friction formula in terms of the mean velocity $\bar{u}$ instead of U, to conform to the ordinary friction formula of a steady channel flow for large values of $\hat{U}/\sigma H)$. This case was already discussed in Paper [1].

To solve (2-1) in an explicit form, we need to have another equation connecting the velocity u and the stress τ. If we introduce the vertical eddy viscosity K_z by

$$K_z \frac{\partial u}{\partial z}=\frac{\tau}{\rho}, \tag{2-30}$$

the combination of (2-1) and (2-30) gives the basic equation

$$\frac{\partial^2 u^*}{\partial z^2}-\frac{i\sigma}{K_z}u^*=0, \tag{2-31}$$

where τ/ρ is replaced by u^* with the aid of (2-16).

For the case of a laminar oscillatory motion in deep water, K_z is the molecular kinematic viscosity ν and the solution of (2-31) with the condition (2-3b) is given by

$$u^*/u_B^*=e^{-\beta L z}. \tag{2-32}$$

where

$$\beta_L=\sqrt{\sigma/\nu}e^{i\pi/4}. \tag{2-33}$$

In terms of velocity u and the outer velocity U, we have, from (2-30), (2-32) and (2-3a),

$$(U-u)/U=e^{-\beta_L z}, \tag{2-34}$$

and

$$\tau_B/\rho=U(\sigma\nu)^{1/2}e^{i\pi/4}. \tag{2-35}$$

The wave displacement thickness δ^* now becomes

$$\delta^*=\delta_L=\sqrt{\nu/\sigma}. \tag{2-36}$$

With a Reynolds number R defined by

$$R=\hat{U}\delta_L/\nu, \tag{2-37}$$

the friction coefficient C derived from (2-19) and (2-35) is

$$C=e^{i\pi/4}/R. \tag{2-38}$$

If we consider that the important quantities, related to the bottom frictional processes in deep water for the case of a smooth bottom, are $\hat{U}$, σ, and ν, dimensional analysis indicates that the friction coefficient C in the turbulent case, too, can be expressed as a function of R alone. For the case of a rough bottom, we usually introduce some length scale D and neglect ν, so that the friction coefficient is expected to be given by a function of $\hat{U}/(\sigma D)$. To find the explicit functional form for C, we have to assume a suitable K_z. This will be done in the next section where the assumptions on K_z applicable to the case of a steady turbulent flow are translated into the mean state of the oscillatory turbulent flow.

3. Assumptions on the structure of an oscillatory turbulent flow

(a) The case of a smooth bottom

Following the concept of the wall and the defect layers established for the case of a steady turbulent boundary layer (see, for example, Clauser, 1956, Mellor and Gibson, 1966), we assume the frictional layer of the oscillatory flow to consist of 3 parts: the inner layer, the overlap layer, and the outer layer. The inner and overlap layers are collectively

called the wall layer in which the direct effect of the bottom boundary is felt, and the overlap and outer layers are the defect layer where the defect velocity profile is governed by the overall characteristics of the frictional layer. The characteristic of the overlap layer is that the velocity profile is expressed by both the wall and the defect forms. In the overlap layer for the case of the steady equilibrium turbulent boundary layer, Prandtl's mixing length theory seems to be applicable (Mellor and Gibson, 1966) so that the eddy viscosity can be written in the form $K_z=k|u_*|z$, with the definition of u_* as $\tau/\rho=|u_*|u_*$. In the outer layer, eddy viscosity is assumed to be proportional to the outer velocity and the displacement thickness. In the inner layer, the effective viscosity varies from the molecular viscosity to the eddy viscosity corresponding to the base of the overlap layer in the range $5\lesssim u_*z/\nu\lesssim 30$ (Mellor, 1966).

In the reformulation from the eddy viscosity assumption valid for the case of steady turbulent flow to the case of oscillatory flow over a smooth bottom, we make some simplifications. Thus, we introduce the thickness D_L of the viscous sub-layer, in a conventional way, by

$$\hat{u}_B^* D_L/\nu=N \quad \text{with} \quad N=\text{const.} \tag{3-1}$$

We neglect the transition region between the viscous sub-layer and the overlap layer, so that, in the present case, the viscous sub-layer and the inner layer are identical. The eddy viscosity K_z then assumes the form:

$$K_z=\begin{cases}\nu, & \text{for} \quad 0\leq z<D_L, & \text{(3-2a)}\\ k\hat{u}_B^* z, & \text{for} \quad D_L<z\leq d, & \text{(3-2b)}\\ K_d, & \text{for} \quad d\leq z<\delta, & \text{(3-2c)}\end{cases}$$

and

$$K_d=k\hat{u}_B^* d=K\hat{U}\delta^*, \tag{3-2d}$$

where k and K are universal constants and d is the upper limit of the overlap layer. Although we have no reliable information on N, k, and K for oscillatory turbulent flow, we tentatively assume

$$N=12, \quad k=0.4, \quad \text{and} \quad K=0.02, \tag{3-3}$$

which may be compared with those for the case of steady turbulent flow: $N=11.6$, $k=0.41$, $K=0.016$. Transforming (3-2d) by making use

of (2-27a, b), we have

$$d/\Delta = K/k = 0.05. \tag{3-4}$$

The critical condition, when the overlap layer disappears ($D_L=d$) is given by $R^2=(kN)/(K\hat{C})$, and the formal substitution of (2-38) yields $R=240$.

At this point, it is remarked that if the variation of stress with height is taken into account, it might be better to replace $\hat{u}_B^*$ in (3-1) and (3-2b, d) by the modified friction velocity $\hat{u}^*$ with the definition $\tau/\rho=\hat{u}^*u^*$ instead of (2-16). However, this modification has not been attempted because of the uncertainty of the analogy of the eddy viscosity assumptions between steady flow and oscillatory flow. It is expected that when the thickness of the frictional layer becomes comparable to the thickness of the viscous sub-layer, the results obtained on the assumptions of (3-1), and (3-2a, b, c, d) are somewhat different from those derived from the modified version of the eddy viscosity assumptions. Also, the assumption (3-2d) in the outer layer is only the first approximation, and in reality the eddy viscosity may vary with height following some unknown law.

(b) THE CASE OF A ROUGH BOTTOM

For the case of a rough bottom, the eddy viscosity in the defect layer is the same as for the case of a smooth bottom, but, in the wall layer, we introduce the roughness length z_0 (or Nikuradse's equivalent sand roughness D, $D=30z_0$), although, in reality, the equivalent roughness D is not well understood physically. There is also a question about the origin of the vertical coordinate, namely, the level of the equivalent bottom surface.

If we follow the ordinary formulation of the eddy viscosity in the wall layer, the overlap layer extends to $z=z_0$, and K_z is given by

$$K_z=k\hat{u}_B^*z, \quad \text{for} \quad z_0\leq z\leq d. \tag{3-5}$$

This eddy viscosity assumption is expected to be adequate for the case $(\delta^*/D)^2\gg 1$. However, to include the case when $(\delta^*/D)^2\leq 1$, we assume the alternative form of the eddy viscosity as follows:

$$K_z=\begin{cases}\alpha k\hat{u}_B^*D_R, & \text{for} \quad 0\leq z<D_R, \quad \text{(inner layer)}, \qquad \text{(3-6a)}\\ k\hat{u}_B^*z, & \text{for} \quad D_R<z\leq d, \quad \text{(overlap layer)}, \qquad \text{(3-6b)}\end{cases}$$

where D_R is the height of the inner layer in which the eddy viscosity is constant. From the requirement that, for $(\delta^*/D)^2 \gg 1$, the velocity profile above D_R derived on the assumption (3-6a, b) coincides with that derived on the assumption (3-5), we take (see § 4, (4-40))

$$1/\alpha = \ln (D_R/z_0). \tag{3-7}$$

Furthermore, since the inner layer exists in a statistical sense only because of the presence of roughness elements, we assume

$$D_R = D/2 = 15z_0, \tag{3-8}$$

and, consequently, it follows

$$1/\alpha = \ln 15 = 2.708. \tag{3-9}$$

For small values of δ^*/D_R, the friction coefficient is essentially governed by K_z in the inner layer, so that, by replacing ν in (2-38) by $\alpha k \hat{u}_B^* D_R$, we have

$$C = (\alpha k \sigma D_R/\hat{U})^{2/3} e^{i\pi/4}. \tag{3-10}$$

Roughly speaking, the range of applicability of (3-10) is given by $\delta^*/D_R < 1$ which can be transformed, by means of (3-10), into $\hat{U}/(\sigma D_R) < (\alpha k)^{-2}$, and the substitution of numerical values yields $\hat{U}/(\sigma z_0) < 685$.

On the other hand, the condition of the vanishing overlap layer is given by $\hat{U}/(\sigma D_R) < k/K\hat{C}^{1/2})$, and taking (3-10) into account, we may estimate the critical value of $\hat{U}/(\sigma z_0)$ somewhere around 10^3. The delineation of various flow regimes, such as the smooth or rough bottoms, and the viscous or turbulent flows will be discussed later (see § 5, (c)).

4. Derivation of the velocity profile and the friction coefficient

(a) THE CASE OF A SMOOTH BOTTOM

The substitution of the eddy viscosity assumption (3-2a, b, c) into (2-31) yields

$$\frac{\partial^2 u^*}{\partial z^2} - \frac{i\sigma}{\nu} u^* = 0, \quad \text{for} \quad 0 \leq z < D_L, \tag{4-1a}$$

$$\frac{\partial^2 u^*}{\partial z^2} - i\left(\frac{\sigma}{k\hat{u}_B^* z}\right) u^* = 0, \quad \text{for} \quad D_L < z \leq d, \tag{4-1b}$$

and

$$\frac{\partial^2 u^*}{\partial z^2}-\frac{i\sigma}{K_d}u^*=0, \quad \text{for} \quad d\leq z<\delta. \tag{4-1c}$$

For the deep water case when the bottom frictional layer is very thin compared with the total depth of water, the boundary conditions at the bottom and the outer edge of the frictional layer are

$$u=0 \quad \text{at} \quad z=0, \tag{4-2a}$$

$$u^*\to 0 \quad \text{as} \quad z\to\infty. \tag{4-2b}$$

The conditions between the inner and overlap layers at $z=D_L$ and between the overlap and outer layers at $z=d$ are determined by the continuity of u and u^*. However, the continuity of u may be replaced by the continuity of $\partial u^*/\partial z$ in view of equation (2-1), so that we put

$$u^*,\ \partial u^*/\partial z \quad \text{continuous at} \quad z=D_L,\ z=d. \tag{4-3}$$

In the inner layer, a solution of (4-1a) is given by

$$u^*/u_L^*=A\sinh\beta_L(D_L-z)+\cosh\beta_L(D_L-z), \tag{4-4}$$

where A is an integration constant, $\beta_L=\sqrt{\sigma/\nu}e^{i\pi/4}$ and the suffix L denotes the quantity at $z=D_L$. Then (2-30) yields

$$\begin{aligned} u/u_L^*=\hat{u}_B^*/(\nu\beta_L)[&\sinh\beta_L D_L-\sinh\beta_L(D_L-z)\\ &+A\{\cosh\beta_L D_L-\cosh\beta_L(D_L-z)\})], \end{aligned} \tag{4-5}$$

where the boundary condition (4-2a) is taken into account.

In the outer layer, a solution of (4-1c) with the condition (4-2b) is given by

$$u^*/u_d^*=e^{-\beta_d(z-d)}, \tag{4-6}$$

where $\beta_d=\sqrt{\sigma/K_d}e^{i\pi/4}$ and the suffix d denotes the quantity at $z=d$. From (2-30), then, the velocity u is

$$(U-u)/u_d^*=\{\hat{u}_B^*/(K_d\beta_d)\}\,e^{-\beta_d(z-d)}, \tag{4-7}$$

where U is the reference velocity outside the frictional layer.

In the overlap layer, it is convenient to change the independent variable z to y defined by

$$y^2=(4z)/(k\Delta)=(4\sigma z)/(k\hat{u}_B^*), \tag{4-8}$$

where Δ is defined by (2-18). Then, (4-1b) is reduced to Bessel's differential equation and the solution can be written as

$$\frac{u^*}{u_a^*}=\frac{yZ_1(y,\ c)}{y_aZ_1(y_a,\ c)}, \tag{4-9}$$

where $y=ye^{-i\pi/4}$, and the suffix a denotes the quantity at $z=a$ within the overlap layer. In later use of (4-9), we put $a=d$ or D_L according to the situation and, in particular, D_L is abbreviated by L when used as a suffix. It is mentioned here that the substitution of (3-4) into (4-8) yields

$$y_d^2=4K/k^2. \tag{4-10}$$

$Z_n(y,\ c)$ is a cylindrical function defined by

$$Z_n(y,\ c)=cJ_n(y)+H_n^{(2)}(y), \tag{4-11}$$

where $J_n(y)$ and $H_n^{(2)}(y)$ are the Bessel function and the Hankel function of the second kind of order n, respectively and $c(=c_1+ic_2)$ is a complex constant. $Z_n(y,\ c)$, for $n=0,\ 1$, satisfies the following relations:

$$\frac{d}{dy}\{Z_0(y,\ c)\}=-Z_1(y,\ c), \tag{4-12a}$$

$$\frac{d}{dy}\{yZ_1(y,\ c)\}=yZ_0(y,\ c). \tag{4-12b}$$

For small values of $y(y^2/4\ll 1)$, $Z_n(y,\ c)$ may be approximated by

$$Z_0(y,\ c)=c_1+ic_2+\frac{1}{2}-i\left(\frac{2}{\pi}\right)\left(\gamma+\ln\frac{y}{2}\right), \tag{4-12c}$$

$$Z_1(y,\ c)=i\left(\frac{2}{\pi}\right)\Big/y, \tag{4-12d}$$

where $\gamma=0.5722\cdots$ (Euler's constant).

The velocity u is obtained by the substitution of (4-9) into (2-30) with a suitable change of variables. With u_a as the velocity at the level $z=a$, we have

$$\frac{u-u_a}{u_a^*}=\left(\frac{2}{k}\right)\left\{\frac{Z_0(y_a,\ c)-Z_0(y,\ c)}{y_aZ_1(y_a,\ c)}\right\}. \tag{4-13}$$

Applying the boundary conditions (4-3) at $z=d$ to (4-6) and (4-9) with $a=d$, the constant of integration c can be determined by the following equation

$$Z_1(y_d, c)=iZ_0(y_d, c). \tag{4-14}$$

Substituting u_d/u_d^* derived from (4-7) into (4-13) with $a=d$, replacing $\hat{u}_B^*/(K_d\beta_d)$ by its equivalent expression $-2i/(ky_d)$, and taking (4-14) into account, we may derive, in the overlap layer,

$$\frac{U-u}{u_a^*}=\left(\frac{2}{k}\right)\frac{Z_0(y, c)}{y_aZ_1(y_a, c)}. \tag{4-15}$$

Now, applying the boundary conditions (4-3) at $z=D_L$ to (4-4) and (4-9) with $a=D_L$, we have

$$A=(\nu\beta_L/\hat{u}_B^*)B, \tag{4-16a}$$

with

$$B=\left(\frac{2}{k}\right)\frac{Z_0(y_L, c)}{y_LZ_1(y_L, c)}, \tag{4-16b}$$

and the substitution of u_L/u_L^* obtained from (4-5) into (4-15) with $a=D_L$, yields

$$U/u_L^*=\frac{\hat{u}_B^*}{(\nu\beta_L)}(\sinh\beta_LD_L+A\cosh\beta_LD_L). \tag{4-17}$$

It should be noticed that if the eddy viscosity K_d in the outer layer is assumed in the form of (3-2d) even after the overlap layer disappears, we can derive the same equation as (4-17) from (4-4) and (4-7), provided that

$$B=e^{-i\pi/4}/\sqrt{K}. \tag{4-18}$$

From (4-4) with $z=0$ and (4-17), it follows

$$\frac{u_B^*}{U}=\left(\frac{\nu\beta_L}{\hat{u}_B^*}\right)\left(\frac{A\tanh\beta_LD_L+1}{\tanh\beta_LD_L+A}\right). \tag{4-19}$$

Now, since we may put

$$\beta_LD_L=\frac{\sqrt{kN}}{2}y_Le^{-i\pi/4}, \quad \frac{\nu\beta_L}{\hat{u}_B^*}=\frac{1}{2}\sqrt{\frac{k}{N}}y_Le^{i\pi/4}, \tag{4-20}$$

we can express the friction coefficient given by (2-22) in the form

$$\hat{C}^{1/2}e^{i\theta}=u_B^*/U=L(y_L). \tag{4-21}$$

On the other hand, the Reynolds number R defined by (2-37) can be expressed as

$$R=(4N/k)^{1/2}(\hat{C}^{1/2}y_L)^{-1}. \tag{4-22}$$

Therefore, we may compute the friction coefficient C as a function of R alone.

The formula (4-19) may be simplified for two limiting cases; namely, i) $\tanh\beta_L D_L\to 1$ and ii) $\tanh\beta_L D_L\to\beta_L D_L$. The range of transition in terms of δ_L/D_L from the condition i) to ii) is approximately given by

$$0.5\lesssim\delta_L/D_L\lesssim 2. \tag{4-23}$$

This condition can be interpreted that if the main part of the frictional layer is in the viscous sub-layer, the frictional law reverts to the laminar law. Indeed, for large values of $\beta_L D_L$ (small values of δ_L/D_L), (4-19) is reduced to

$$u_B^*/U=\nu\beta_L/\hat{u}_B^*, \tag{4-24}$$

which is equivalent to (2-38) derived for the case of a laminar flow.

For small values of $\beta_L D_L$ (large values of δ_L/D_L), (4-4) and (4-19) are approximated by

$$u^*/u_L^*=1, \quad \text{for} \quad 0\leq z<D_L, \tag{4-25}$$

$$u_B^*/U=(N+B)^{-1}, \tag{4-26}$$

where N and B are given by (3-1) and (4-16b) respectively. Furthermore, in this case, we may approximate B by

$$B=\frac{\pi}{k}\left\{c_2-\left(\frac{2}{\pi}\right)\left(\gamma+\ln\frac{y_L}{2}\right)-i\left(c_1+\frac{1}{2}\right)\right\}, \tag{4-27}$$

with the aid of (4-12c, d). Thus, the friction coefficient is given by

$$1/\hat{C}=\left(\frac{2}{k}\right)^2\left\{\left(P-\ln\frac{y_L}{2}\right)^2+Q^2\right\}, \tag{4-28a}$$

$$\tan\theta=Q\Big/\left(P-\ln\frac{y_L}{2}\right), \tag{4-28b}$$

where

$$P=\frac{k}{2}N+\frac{\pi}{2}c_2-\gamma, \tag{4-29a}$$

$$Q=\frac{\pi}{2}\left(c_1+\frac{1}{2}\right). \tag{4-29b}$$

These formulas (4-28a, b) are analogous to those given in Paper [1], (5-8), where the approximations of (4-25) and (4-27) were made from the beginning and c_1 and c_2 were neglected.

If y_L is very small, further simplification of (4-28a, b) is possible. By neglecting Q^2 compared with $(P-\ln y_L/2)^2$, we have

$$1/\hat{C}^{1/2}=\left(\frac{2}{k}\right)\left(P-\ln\frac{y_L}{2}\right), \tag{4-30a}$$

$$\theta=Q\Big/\left(P-\ln\frac{y_L}{2}\right). \tag{4-30b}$$

Taking (4-22) into account, we may transform (4-30a) into

$$\frac{k}{2\hat{C}^{1/2}}+\ln\left(\frac{1}{\hat{C}^{1/2}}\right)=P+\frac{1}{2}\ln\left(\frac{k}{N}\right)+\ln R. \tag{4-31}$$

(b) THE CASE OF A ROUGH BOTTOM

The difference of a rough bottom from a smooth bottom lies in the eddy viscosity assumption in the inner layer. Thus, the discussions for the case of a smooth bottom can be translated into the case of a rough bottom by the following transformation in (4-4), (4-5), (4-16a, b), (4-17) and (4-19):

$$\hat{u}_B^*/(\nu\beta_L)\to 2/(\sqrt{\alpha}\,ky_Re^{i\pi/4}), \tag{4-32a}$$

$$\beta_L D_L\to y_Re^{i\pi/4}/(2\sqrt{\alpha}), \tag{4-32b}$$

$$y_L\to y_R, \tag{4-32c}$$

where the suffix R denotes the quantity at $z=D_R$. Thus, in place of (4-21) and (4-22), we have

$$\hat{C}^{1/2}e^{i\theta}=L(y_R), \tag{4-33}$$

$$\hat{U}/(\sigma D_R)=4/(k\hat{C}^{1/2}y_R^2), \tag{4-34}$$

and $L(y_R)$ is obtained from $L(y_L)$ by the transformation

$$N\to 1/(\alpha k),\quad y_L^*\to y_R^*. \tag{4-35}$$

(4-33) and (4-34) show that the friction coefficient C can be computed as a function of $\hat{U}/(\sigma D_R)$ alone.

In particular, for large and small values of $y_R^*/(2\sqrt{\alpha})$, approximate formulas become

$$u_B^*/U=\sqrt{\alpha}\,ky_R^*/2, \tag{4-36}$$

$$u_B^*/U=\{1/(\alpha k)+B\}^{-1}, \tag{4-37}$$

in place of (4-24) and (4-26) respectively, and (4-36) is now equivalent to (3-10) as is expected.

If the ordinary eddy viscosity assumption (3-9) is adopted, we have, in general, from (4-15),

$$u_B^*/U=1/B, \tag{4-38}$$

where B should be evaluated at y_B, namely, at $z=z_0$, instead of at y_R(or $z=D_R$). Since we assume that, for small values of $y_R^*/(2\sqrt{\alpha})$, (4-37) is equivalent to (4-38), we have the condition

$$1/(\alpha k)+B(y_R)=B(y_B). \tag{4-39}$$

The substitution of the approximate formula for B into (4-39) yields

$$1/\alpha=2\ln(y_R/y_B)=\ln(D_R/z_0), \tag{4-40}$$

which is the condition for α assumed in (3-7). Taking this condition into consideration, the friction coefficient C can be written in the form (4-28a, b), provided that y_L is replaced by y_B and P by P' where

$$P'=(\pi/2)c_2-\gamma. \tag{4-41}$$

This, in turn, means that the friction coefficient for the case of a smooth bottom can be expressed by the formula for a rough bottom, if we put

$$P-\ln(y_L/2)=P'-\ln(y_B/2). \tag{4-42}$$

Taking (4-29a) and (4-41) into account, (4-42) becomes

$$\ln(y_B/y_L)=-kN/2. \tag{4-43}$$

Thus, the equivalent roughness D for the smooth bottom with the

laminar thickness D_L is given by

$$D=(30e^{-kN})D_L=0.366D_L. \tag{4-44}$$

If y_B is very small, we can deduce the equations similar to (4-30a, b) for a rough bottom. Taking (4-34) into account, it follows,

$$\frac{k}{\hat{C}^{1/2}}+\ln\left(\frac{1}{\hat{C}^{1/2}}\right)=\ln s+\ln\left(\frac{\hat{U}}{\sigma z_0}\right), \tag{4-45}$$

where

$$\ln s=2P'+\ln k. \tag{4-46}$$

The formula for the length scale Δ given by (2-27b) can be derived easily from (4-45) as

$$(s\Delta/z_0)\ln(s\Delta/z_0)=sk\hat{U}/(\sigma z_0). \tag{4-47}$$

It is mentioned here that (4-45) and (4-47) are analogous to the semi-empirical formulas proposed by Jonsson (1963) for the friction coefficient and the boundary layer thickness[2] (see § 6, (a) ii). Futhermore, for the derivation of the friction formula for a smooth bottom, Jonsson (1967) assumed $D\sim 0.435D_L$ in place of (4-44).

5. Numerical results

(a) VERTICAL DISTRIBUTIONS OF SHEAR STRESS AND VELOCITY

At first, let us summarize the principal results of the preceding section for the case of a smooth bottom and express them in terms of

2) In particular, the wave boundary layer thickness "δ" defined by Jonsson is

$$(\text{“}\delta\text{”}/z_0)\log(\text{“}\delta\text{”}/z_0)=1.2\hat{U}/(\sigma D). \tag{B-1}$$

Transforming (4-47) in the form of (B-1), we have, with constant factor n,

$$(ns\ln 10)(\Delta/z_0)[\log\{(n\ln 10)(\Delta/z_0)\}-\log(n\ln 10)]=nsk\times 30\hat{U}/(\sigma D). \tag{B-2}$$

Neglecting the second term in the bracket in the left hand side as small, we have, by comparison of (B-1) and (B-2),

$$(ns\ln 10)\Delta=\text{“}\delta\text{”}, \tag{B-3}$$

$$30nsk=1.2. \tag{B-4}$$

Since $k=0.4$, (B-4) yields $ns=0.1$ and (B-3) becomes

$$0.23\Delta=\text{“}\delta\text{”}. \tag{B-5}$$

y and y_L for the convenience of numerical computation. The universal constants, k, K, N, and consequently y_d are assumed known.

With reference to the bottom friction velocity u_B^*, the vertical distribution of stress given by (4-4), (4-6), and (4-9) are written, with the aid of (4-16 a, b) and (4-20), as

$$u^*/u_B^* = \begin{cases} S(y_L, y)/S(y_L, 0), & \text{for } 0 \leq y \leq y_L, \quad (5\text{-}1a) \\ G(y_L)F_1(y), & \text{for } y_L \leq y, \quad (5\text{-}1b) \end{cases}$$

where

$$S(y_L, y) = A(y_L) \sinh \{ny_L^*(1-y^2/y_L^2)\} + \cosh \{ny_L^*(1-y^2/y_L^2)\}, \quad (5\text{-}2a)$$

$$G(y_L) = \{S(y_L, 0)y_L Z_1(y_L)\}^{-1}, \quad (5\text{-}2b)$$

$$F_1(y) = \begin{cases} yZ_1(y), & \text{for } y_L \leq y \leq y_d, \quad (5\text{-}2c) \\ y_d Z_1(y_d) \exp[(y_d^*/2)(1-y^2/y_d^2)], & \text{for } y_d \leq y, \quad (5\text{-}2d) \end{cases}$$

$$A(y_L) = my_L^*(2/k)Z_0(y_L)/\{y_L Z_1(y_L)\}, \quad (5\text{-}2e)$$

and

$$m = \frac{1}{2}\sqrt{\frac{k}{N}}, \qquad n = mN = \sqrt{kN}/2,$$

$$y_L = y_L e^{-i\pi/4}, \quad y_L^* = y_L e^{i\pi/4}, \quad y_d = 2\sqrt{K}/k. \quad (5\text{-}2f)$$

The corresponding velocity distribution given by (4-5), (4-7) and (4-15) can be transformed into

$$\frac{U-u}{u_B^*} = \begin{cases} 1/(my_L^*)[T(y_L, y)/S(y_L, 0)], & \text{for } 0 \leqslant y \leqslant y_L, \quad (5\text{-}3a) \\ (2/k)G(y_L)F_2(y), & \text{for } y_L \leq y, \quad (5\text{-}3b) \end{cases}$$

where

$$T(y_L, y) = \sinh \{ny_L^*(1-y^2/y_L^2)\} + A(y_L) \cosh \{ny_L^*(1-y^2/y_L^2)\}, \quad (5\text{-}4a)$$

$$F_2(y) = \begin{cases} Z_0(y), & \text{for } y_2 \leqslant y \leqslant y_d, \quad (5\text{-}4b) \\ Z_0(y_d) \exp[(y_d^*/2)(1-y^2/y_d^2)], & \text{for } y_d \leqslant y. \quad (5\text{-}4c) \end{cases}$$

If y_d is smaller than y_L, the overlap layer vanishes and the stress and velocity distribution in the outer layer, $y_L \leq y$, given by (4-6), and (4-7), together with (4-18), become

$$u^*/u_B^* = \exp[y_L^2/(2y_d)(1-y^2/y_L^2)]/S(y_L, 0), \quad (5\text{-}5a)$$

$$(U-u)/u_B^*=\exp\left[y_L^2/(2y_d)(1-y^2/y_L^2)-i\pi/4\right]/(\sqrt{K}S(y_L,0)). \tag{5-5b}$$

For the case of a rough bottom, similar expressions can be given by replacing y_L by y_R. In this case, the definition of m and n in (5-2f) should be replaced by

$$m=k\sqrt{\alpha}/2, \quad n=1/(2\sqrt{\alpha}), \quad N\to 1/(\alpha k). \tag{5-6}$$

To compute $Z_n(y)$, $n=1, 2$, defined by (4-11), we need numerical values of $J_n(y)$, $H_n^{(2)}(y)$, and c. $J_n(y)$ and $H_n^{(2)}(y)$ may be found, for example, in the "Table of Functions" by Jahnke and Emde (1945), pp 244-268, where $J_n(y^*)$ and $H_n^{(2)}(y^*)$ are given. For small values of y, $Z_n(y)$ can be approximated by (4-11c, d). The constant $c(=c_1+ic_2)$ determined by the condition (4-14) is shown in Fig. 1 as a function of y, where it is seen that the amplitude $\hat{c}(=\sqrt{c_1^2+c_2^2})$ decreases rapidly with the increase of y, so that for large values of $y_d(y_d\geq 2)$, $Z_n(y)$ may be closely approximated by $H_n^{(2)}(y)$ and y_d does not play an important role in the friction coefficient.

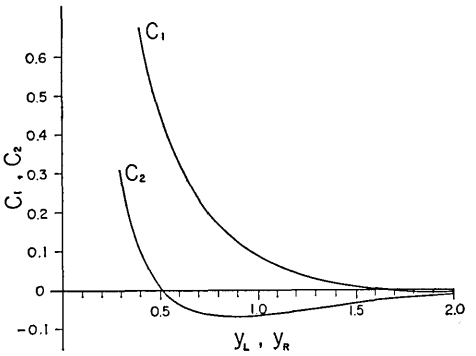

Fig. 1. Constant c $(=c_1+ic_2)$ as a function of y_L or y_R.

In the following computation, we have assumed

$$k=0.4, \quad y_d=0.7, \quad N=12, \quad \alpha=1/(\ln 15), \tag{5-7a}$$

so that it follows from (4-10), and Fig. 1,

$$K=0.0196, \quad c_1=0.2361, \quad c_2=-0.0593. \tag{5-7b}$$

If we look into the profiles of the stress and defect velocity in the defect layer ($y>y_L$ or y_R), the important quantities are $G(y_L)$, $G(y_R)$, $F_1(y)$, and $F_2(y)$, among which G may be called the profile factor and F_1 and F_2 are the universal profiles of the shear stress and the defect velocity, respectively. The amplitudes $\hat{G}$ and phases ϕ of the profile factors $G(y_L)$ and $G(y_R)$ are shown in Fig. 2 as functions of y_L or y_R respectively, where it is seen that the variation of the amplitudes of $G(y_L)$and $G(y_R)$ are relatively small and the deviation from $\pi/2$ is only a few percent

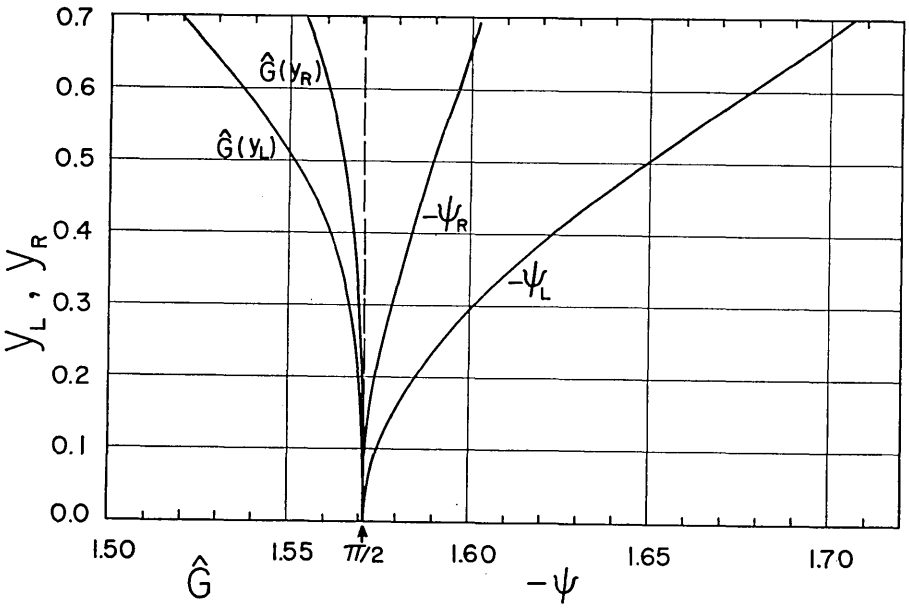

Fig. 2. Amplitudes and phases of $G(y_L)$ and $G(y_R)$ as a function of y_L or y_R, where Phase $[G(y_L)]=\phi_L$, and Phase $[G(y_R)]=\phi_R$.

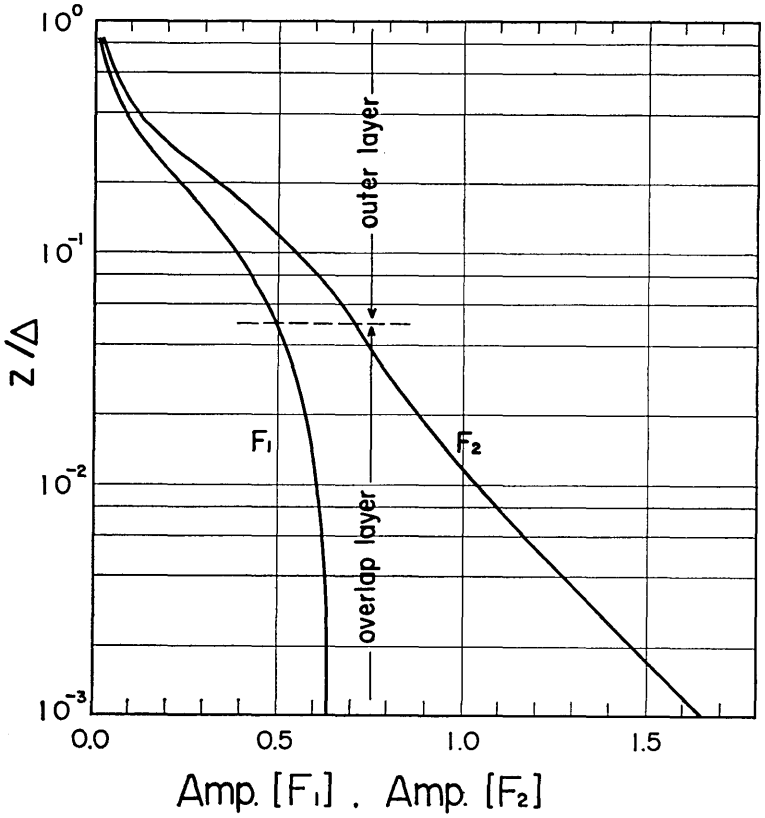

Fig. 3a. Amplitudes of F_1 and F_2 as a function of z/Δ.

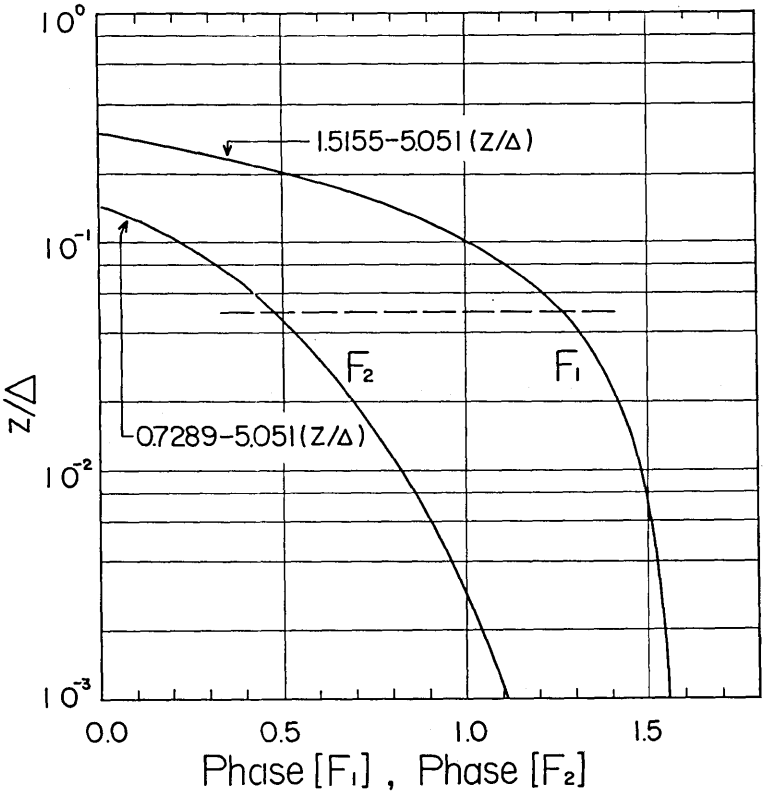

Fig. 3b. Phases of F_1 and F_2 as a function of z/Δ.

even for the condition of y_L or $y_R=y_a$. The universal profiles $F_1(y)$ and $F_2(y)$ are shown in Fig. 3a, b where the amplitudes and phases are shown as a function of $z/\Delta(=y^2/10)$. It is seen that, in the lower part of the overlap layer, the variation of $F_1(y)$ is small and the corresponding variation of $F_2(y)$ is logarithmic. In the outer layer, $F_1(y)$ and $F_2(y)$ are given explicitly by

$$F_1(y)=0.6336e^{i(1.5155)}\cdot\exp\{(1+i)\cdot 5.051\cdot(z/\Delta)\}, \tag{5-8a}$$

and

$$F_2(y)=0.9044e^{i(0.7289)}\cdot\exp\{(1+i)\cdot 5.051\cdot(z/\Delta)\}. \tag{5-8b}$$

If the overlap layer vanishes, the stress and defect velocity are given by (5-5a) and (5-5b) respectively, and it is found that the profiles with

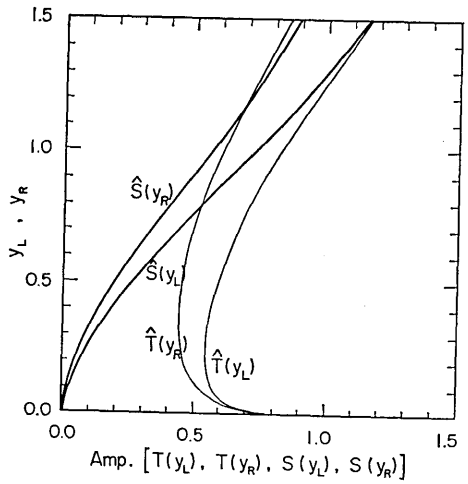

Fig. 4a. Amplitudes of $T(y_L)$, $T(y_R)$, $S(y_L)$ and $S(y_R)$ as a function of y_L or y_R.

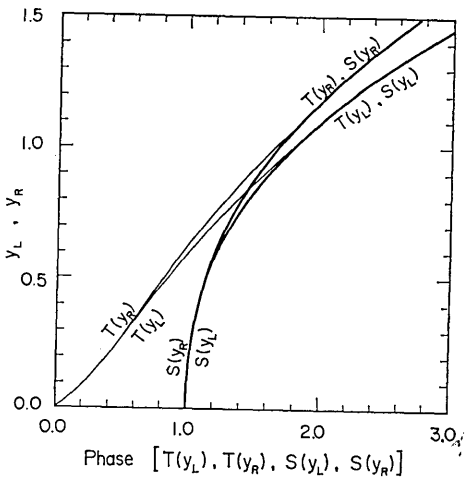

Fig. 4b. Phases of $T(y_L)$, $T(y_R)$, $S(y_L)$ and $S(y_R)$ as a function of y_L or y_R.

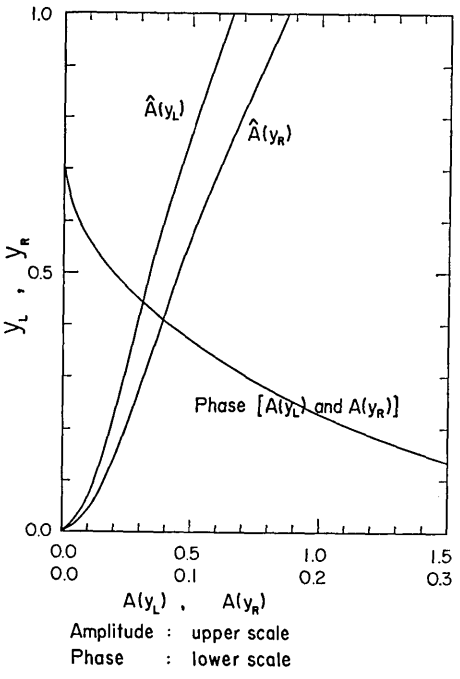

Fig. 5. Amplitudes and phases of $A(y_L)$ and $A(y_R)$ as a function of y_L or y_R.

respect to z/Δ are the same as (5-8a), (5-8b), apart from the constant factors depending on y_L or y_R.

The amplitudes and phases of the factors $S(y_L, 0)$, $S(y_R, 0)$, $T(y_L, 0)$, and $T(y_R, 0)$ are shown in Fig. 4a, b as functions of y_L or y_R, where it is seen that for small values of y_L and y_R, pairs of $S(y_L, 0)$ and $S(y_R, 0)$, $T(y_L, 0)$ and $T(y_R, 0)$ coincide and, for large values of y_L and y_R, pairs of $S(y_L, 0)$, and $T(y_L, 0)$, $S(y_R, 0)$ and $T(y_R, 0)$ coincide with each other. $A(y_L)$ and $A(y_R)$ are shown in Fig. 5 for the convenience of computing $S(y_L, y)$, $S(y_R, y)$, $T(y_L, y)$, and $T(y_R, y)$, where phases of $A(y_L)$ and $A(y_R)$ are equal for the same values of y_L and y_R.

(b) FRICTION COEFFIENT

From (5-3a) and (4-21) the friction coefficient C for the case of a smooth bottom is given by

$$\hat{C}^{1/2}e^{i\theta}=L(y_L)=my_L^*S(y_L, 0)/T(y_L, 0), \tag{5-9a}$$

and the Reynolds number R is expressed by

$$R=1/(\hat{C}^{1/2}my_L). \tag{5-9b}$$

For the case of a rough bottom, we have

$$\hat{C}^{1/2}e^{i\theta}=L(y_R)=my_R^*S(y_R, 0)/T(y_R, 0), \tag{5-10a}$$

and the parameter $\hat{U}/(\sigma z_0)$ is given by (4-34), namely

$$\hat{U}/(\sigma z_0)=60/(k\hat{C}^{1/2}y_R^2). \tag{5-10b}$$

In Fig. 6a, b and Fig. 7a, b, the friction coefficient C for the cases of smooth and rough bottoms are shown as functions of R and $\hat{U}/(\sigma z_0)$ respectively. In these figures, it is clear that the amplitude $\hat{C}$ and phase θ of the friction coefficient increase with the decrease of the parameters R or $\hat{U}/(\sigma z_0)$, and for small values of these parameters, $\hat{C}=1/R$ for the smooth case and $\hat{C}=1.70\times\{\hat{U}/(\sigma z_0)\}^{-2/3}$ for the rough case with the phase approaching $\pi/4$ in both cases, as is already expected from (2-38) and (3-12). For large values of the parameters R or $\hat{U}/(\sigma z_0)$, the friction coefficient can be calculated easily from (4-31) or (4-42). Here it is remarked that if y_d is assumed to be, say, 1, instead of 0.7, the amplitude of the friction coefficient increases about 10 percent and the phase decreases about 20 percent for large values of the parameters R or $\hat{U}/(\sigma z_0)$.

(c) DELINEATION OF THE FLOW REGIMES

In the case of a steady turbulent pipe flow, a measure of whether the bottom is considered hydrodynamically smooth or rough seems to be given by the ratio D/D_L centered around 1 (Rouse, 1937), and the range of transition may roughly be given by

$$0.4\lesssim D/D_L\lesssim 5. \tag{5-11}$$

According to Colebrook and White (1937), the beginning of transition is

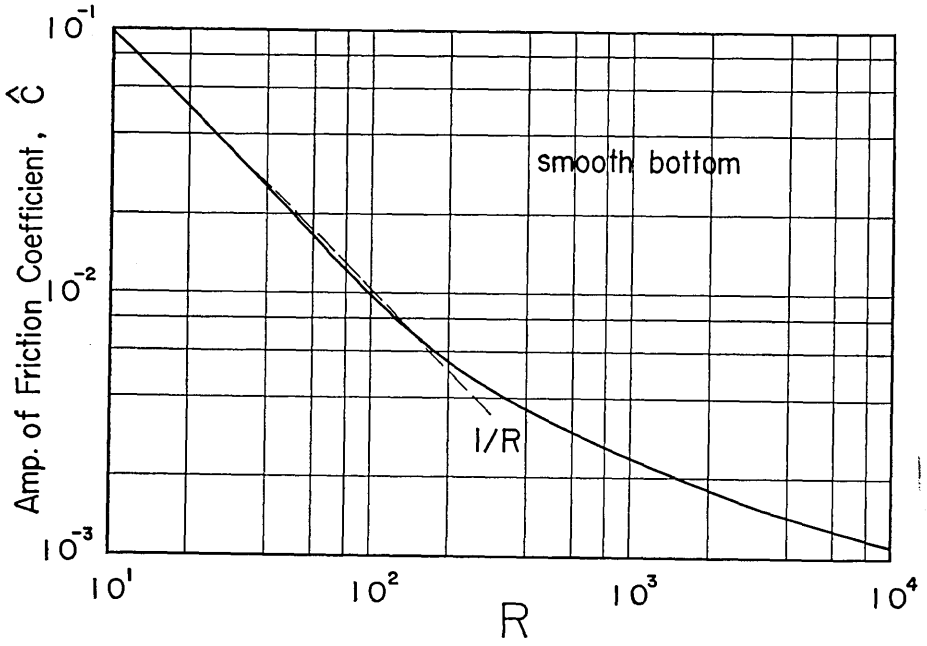

Fig. 6a. Amplitude of friction coefficient, $\hat{C}$, for the case of a smooth bottom, as a function of R.

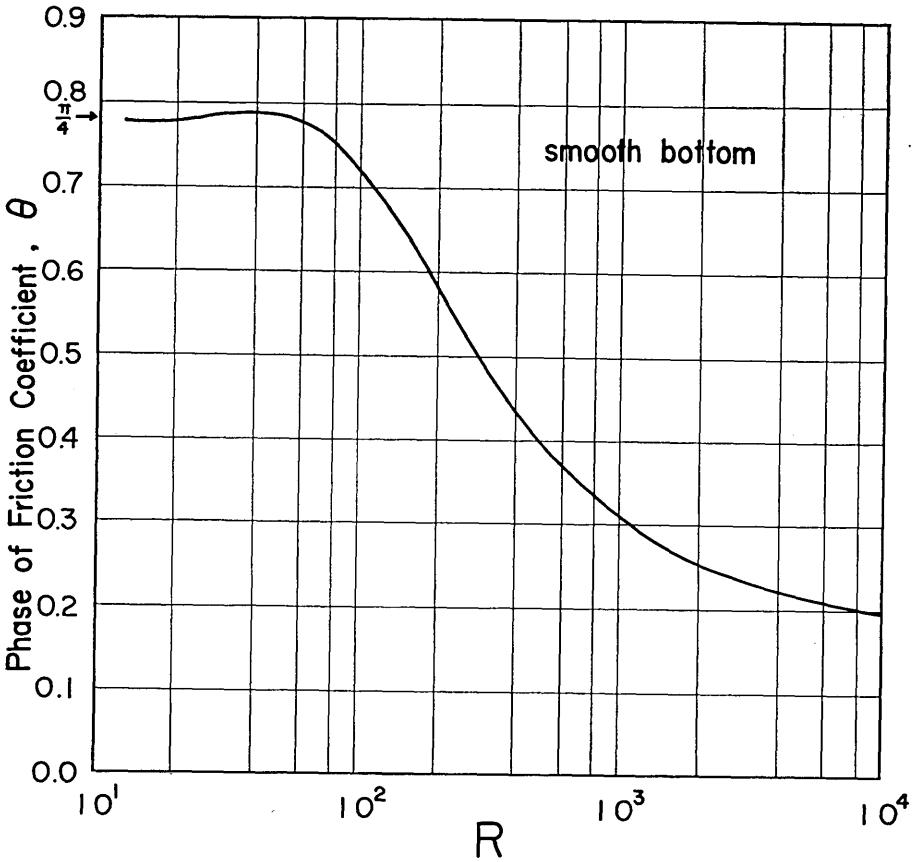

Fig. 6b. Phase of friction coefficient, θ, for the case of a smooth bottom, as a function of R.

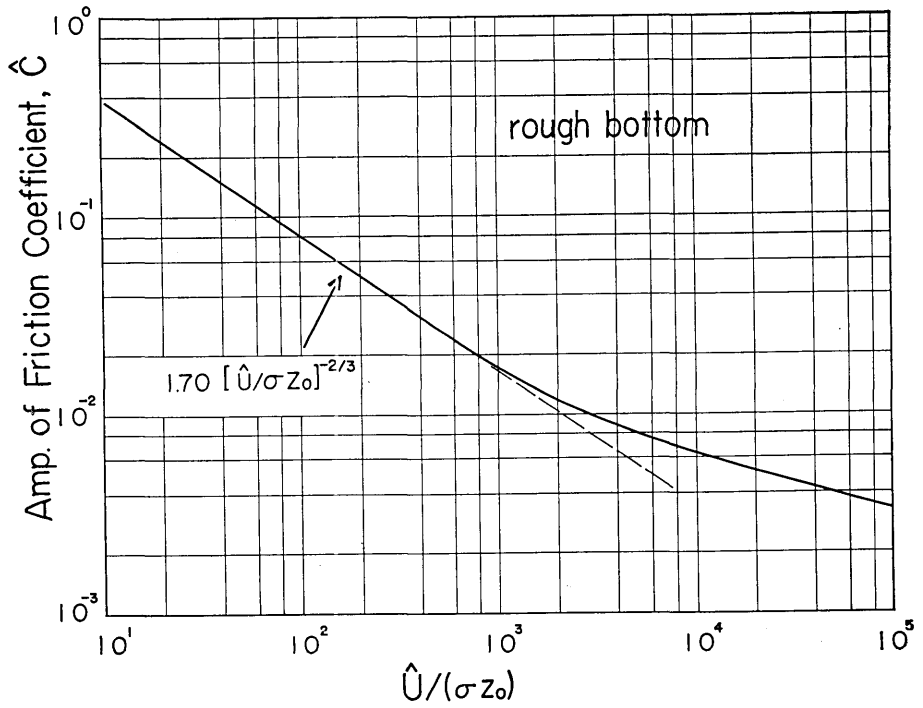

Fig. 7a. Amplitude of friction coefficient, $\hat{C}$, for the case of a rough bottom, as a function of $\hat{U}/(\sigma z_0)$.

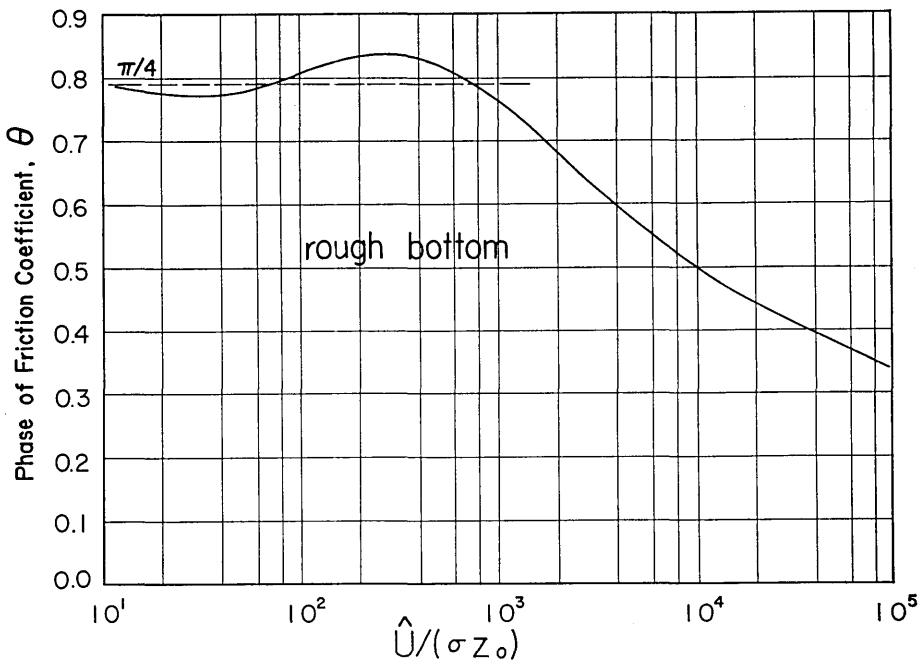

Fig. 7b. Phase of friction coefficient, θ, for the case of a rough bottom, as a function of $\hat{U}/(\sigma z_0)$.

controlled by large grains, so that the lower limit of (5-11) may better be represented by the maximum grain size D_m as $D_m/D_L \sim 0.4$. This is interpreted that if the roughness element is completely submerged in the viscous sub-layer, the bottom is hydrodynamically smooth and if the roughness element is much larger than the thickness of the viscous sub-layer, the bottom is considered rough. In the present formulation, the eddy viscosity in the inner layer (3-10a) becomes equal to the molecular kinematic viscosity ν at $D_R/D_L=(\alpha kN)^{-1}\sim 0.56$. In terms of D, this condition gives $D/D_L\sim 1$ and is consistent with the empirical result for steady turbulent flow (5-10).

For the transition between the viscous and turbulent flows we use similar reasoning, and consider the ratio of the wave displacement thickness δ^* to the thickness of the viscous sub-layer D_L. If $(\delta^*/D_L)^2 \ll 1$, the main part of the frictional layer is submerged in the viscous sub-layer, so that the bottom friction would be governed by a viscous law such as (2-38) for the case of a smooth bottom. Appreciable deviation of the friction coefficient from that governed by a viscous law would be expected if $(\delta^*/D_L)^2 \gg 1$. Therefore, in both smooth and rough bottoms, the transition of the friction coefficient from the laminar type to the turbulent type may be found in some range of δ^*/D_L, say

$$0.4 \lesssim \delta^*/D_L \lesssim 5. \tag{5-12}$$

To show these criteria (5-11) and (5-12) in a figure, it is convenient to write

$$\hat{U}/(\sigma z_0)=30R^2/M, \tag{5-13a}$$

$$M=\hat{U}D/\nu, \tag{5-13b}$$

and express the amplitude of the friction coefficient $\hat{C}$ as a function of R with M as a parameter, as shown in Fig. 8. Then, it is easy to delineate the zones of the smooth-rough, and viscous-turbulent transitions according to (5-10) and (5-12), since we may write

$$D/D_L=\hat{C}^{1/2}M/N, \tag{5-14a}$$

$$\delta^*/D_L=\hat{C}^{3/2}R^2/N. \tag{5-14b}$$

In Fig. 8, it is found that the Reynolds number for the viscous-turbulent transition over a smooth bottom is given by

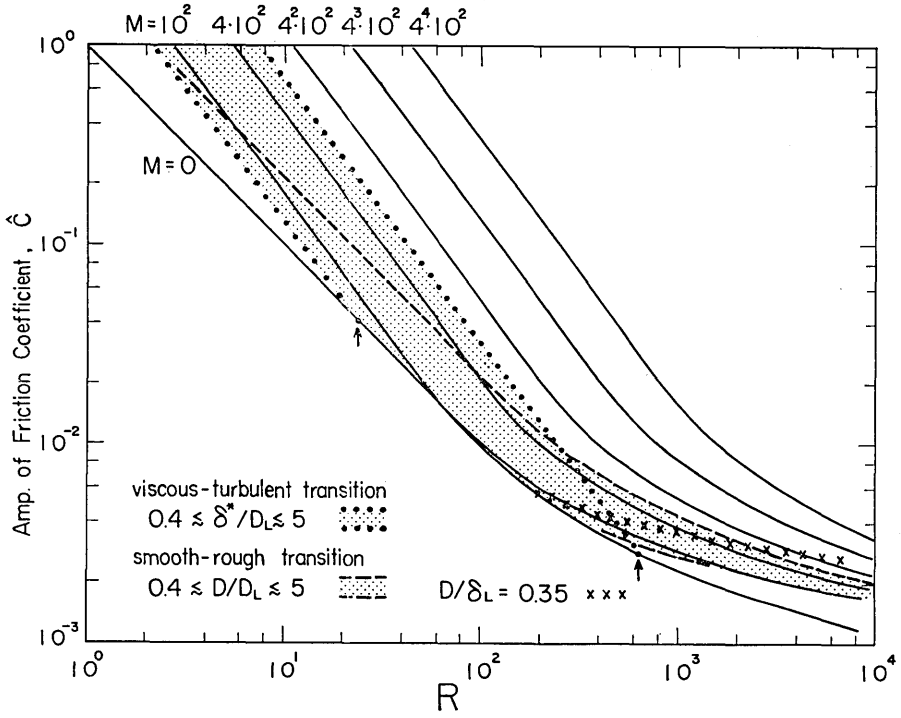

Fig. 8. Delineation of the transitions between laminar and turbulent flows, and between the smooth and rough bottoms. Arrows indicate the transition range between laminar and turbulent flows on a smooth bottom.

$$25 \leq R \leq 650, \tag{5-15}$$

and the critical Reynolds number, $R=113$, determined by Collins (1963) seems to be in the middle of the above range. If we make use of (3-12), we may transform (5-14b), for the condition $\delta^*/D_R<1$, as

$$\delta^*/D_L=\alpha kM/(2N), \tag{5-16}$$

and (5-12) becomes

$$66 \leq M \leq 815. \tag{5-17}$$

On the other hand, Fig. 8 also shows that the relation defined by (5-11) may be roughly approximated by $10^2 \leq M \leq 10^3$ in the range $10^2<R<10^4$. Therefore, from a practical point of view, it appears possible to use

$$10^2 \leq M \leq 10^3 \tag{5-18}$$

as a rough measure for the development of a rough turblent flow in the whole range of R.

For the smooth-rough transition, the condition

$$0.22<D/\delta_L<0.35 \tag{5-19}$$

is sometimes used (Li, 1954, Manohar, 1955). On the R-$\hat{C}$ diagram shown in Fig. 8, it is found that (5-19) is not very different from (5-11), at least in the range $2\times10^2<R<10^3$, so that (5-19) can be used as a criterion of smooth-rough transition in a limited range of R. Jonsson (1957) proposed essentially the same criterion as (5-11).

For the viscous-turbulent transition over a rough bottom, various criteria have been proposed on the basis of experimental data. However, the transition was defined differently and we are not certain which of the criteria proposed so far is most reliable. In terms of the present notations, Li (1954) and Manohar (1955) gave, from their oscillating plate experiments,

$$M=104, \text{ for } 0.22<D/\delta_L<0.35 \tag{5-20a}$$

$$\hat{U}D^{1/5}/\nu=1.55\times10^3, \ (C.G.S. \text{ units}), \text{ for } 0.35<D/\delta_L. \tag{5-20b}$$

Later Kalkanis (1964) criticized the above equations and gave some evidence that

$$M\sim100 \tag{5-20c}$$

for the whole range of the rough bottom. It is interesting to notice that the criterion (5-20c) is near the lower limit of the transition range defined by (5-18).

On the other hand, Vincent (1958) gave the relation

$$\hat{U}D^{1/2}=1.2, \ (C.G.S. \text{ units}), \tag{5-21}$$

from the experiment on progressive waves for the period range of 1 to 5 sec. According to him, the beginning of turbulence over a rough bottom is found for very low values of M, say 15 to 30. If (3-10) is assumed to hold in this limiting case, it may be possible to approximate (5-21) roughly by

$$R_{\delta*}=\hat{U}\delta^*/\nu\sim \text{const.}, \tag{5-22a}$$

since we can transform (5-22a) into

$$\hat{U}D^{1/2}=(R_{\delta*}\cdot\nu)^{3/4}(\alpha k/2)^{-1/2}\sigma^{1/4}. \tag{5-22b}$$

Comparing (5-22b) with (5-21), the value of $R_{\delta*}$ seems to be somewhere around 15 to 20. In terms of R and $\hat{C}$, (5-22a) is written as

$$\hat{C}=R_{\delta*}R^{-2}. \tag{5-22c}$$

Jonsson's criterion (1967) for the fully developed turbulence over a rough bottom is

$$\hat{U}\text{``}\delta\text{''}/\nu=500, \tag{5-23}$$

where "δ" is the height scale of the boundary layer defined by Jonsson and is closely approximated by 0.23Δ of the present paper. Transforming (5-23), we have

$$R_{\Delta}=\hat{U}\Delta/\nu\sim 2.2\times 10^{3}, \tag{5-24a}$$

or, in terms of R and $\hat{C}$,

$$\hat{C}=R_{\Delta}^{2}R^{-4}. \tag{5-24b}$$

If we substitute (3-10) into (5-24b), we may derive

$$\hat{U}D^{1/5}/\nu=(\sigma/\nu)^{2/5}(\alpha k/2)^{-1/5}R_{\Delta}^{3/5}\sim\sigma^{2/5}\times 10^{3}(C.G.S.\text{ units}) \tag{5-24c}$$

which is somewhat similar to the relation (5-20b), if the range of period is around 2 second.

The question of transition between the viscous and turbulent flows over a rough bottom is not settled up to present, but it seems interesting to notice that if (3-10) is assumed to hold, most of the criteria proposed can be approximated by the form

$$\hat{C}\sim\text{const.}\ R^{-n}, \tag{5-25}$$

$$\text{with}\quad n=\begin{cases}4/3\ , & \text{for (5-14b)}\\ 2\ , & \text{for (5-22c)}\\ 4\ , & \text{for (5-20b) and (5-24b).}\end{cases}$$

6. Comparison with experimental data

(a) FRICTION COEFFICIENT

i) Bagnold (1946) gave the drag coefficient "k" from his ingenious

experiments using an oscillating plate. He used artificial ripples with two different pitches ($p=10$ cm, 20 cm) but kept the pitch-height ratio p/h as 6.7/1. The ripple trough sections consist of circular arcs meeting to form sharp crests at an angle of 120°. Similar ripples were examined for a steady turbulent flow by Motzfeld (1937), who gave the equivalent roughness D as $D=4h$. Therefore, we assume the roughness length as $z_0=(4p)/(6.7\times30)\sim0.2$, 0.4 cm. As noticed by Jonsson (1967), the drag coefficient "k" defined by Bagnold corresponds to 1/3 of the ordinary drag coefficient C_f and, from (2-25), $(4/\pi)$ "k" corresponds to $C\cos\theta$. Since the range of Bagnold's experiment was $152.5\times\hat{U}/(\sigma z_0)\geq12.5$, we may compute the theoretical friction coefficient $\hat{C}$ and θ easily from (3-10), where D_R now becomes $2h$. According to Bagnold, "k" becomes almost constant for $\hat{U}/(\sigma p)<1$. This result may be understood by the following model. If we assume the thickness of the inner layer D_R or the equivalent roughness D decreases for $\hat{U}/(\sigma p)<1$ with the decrease of the relative amplitude of the horizontal motion of water $\hat{U}/\sigma$ compared with the ripple pitch p, we may put, in place of (3-6a),

$$K_z=\alpha k\hat{u}_B^* D_R\cdot\hat{U}/(\sigma p),\ \text{for}\ \hat{U}/(\sigma p)<1. \tag{6-1}$$

Substituting this eddy viscosity in place of ν of (2-38), we have, in place of (3-10),

$$\hat{C}=(\alpha k D_R/p)^{2/3}=(2\alpha kh/p)^{2/3}, \tag{6-2}$$

and the phase θ is $\pi/4$. Thus, C becomes constant irrespective of $\hat{U}/(\sigma z_0)$ for $\hat{U}/(\sigma p)<1$, if p/h is kept constant. If relevant numerical values are substituted in (6-2), we have $\hat{C}=0.125$ and $\hat{C}\cos\theta=0.089$.

Table 1. Comparison of the experimental values of $(4/\pi)$ "k" (Bagnold, 1946) with the theoretical prediction.

		$\hat{U}/(\sigma p)>1$					$\hat{U}/(\sigma p)<1$		
$\hat{U}/(\sigma z_0)$		152.5	101.5	76.25	50.75	50	38.13	25	12.5
$\frac{4}{\pi}$"k"	$p=10$ cm ($z_0=0.2$ cm)	0.041	0.056	0.066	—	0.096	—	0.105	—
	$p=20$ cm ($z_0=0.4$ cm)	—	—	0.060	0.092	—	0.097	0.099	0.110
$\hat{C}\cos\theta$	Eq. (3-12)	0.042	0.055	0.067	0.088	0.089	(0.106)	(0.141)	(0.223)
	Eq. (6-2)	—	—	—	—	—	0.089	0.089	0.089

In Table 1, $(4/\pi)$"k" estimated from Fig. 3 of Bagnold's paper is compared with the theoretical estimates where it is seen that the agreement between $(4/\pi)$"k" and $C\cos\theta$ is very good for $\hat{U}/(\sigma p)>1$ and fairly good for $\hat{U}/(\sigma p)<1$.

ii) Jonsson (1963) measured the velocity distribution in a turbulent oscillatory flow over an artificially roughened surface, by making use of the oscillating water tunnel (Test No. 1). The roughness on the bottom surface was provided by a two-dimensional elevation of the triangular shape, 0.6 cm high and 1.7 cm apart. The velocity was measured by a small propeller type current meter of 0.5 cm diameter.

His experimental conditions were $\hat{U}/\sigma=285$ cm, $\hat{U}=211$ cm/sec, $T=\dfrac{2\pi}{\sigma}=8.39$ sec, and from the measured velocity profile, the roughness length was estimated to be $z_0=0.077$ cm. Later, Carlsen (1967) added new data (Test No. 2) on the velocity distribution for the case $\hat{U}/\sigma=179$ cm, $\hat{U}=153$ cm/sec, $T=7.20$ sec, $z_0=0.21$ cm.

The analysis of Jonsson's velocity profile will be given in the next sub-section, but here, in Table 2, the estimates of the friction factor (Jonsson's friction factor is equal to $2\hat{C}$), phase θ, the energy dissipation $<E>$ and the thickness of the wave boundary layer "δ" by Jonsson and Carlsen are compared with the prediction based on the present theory, according to which, $\hat{C}$ and θ can be found as a functiion of $\hat{U}/(\sigma z_0)$, and $<E>/\rho={}^1/_2\hat{C}\hat{U}^3\cos\theta$, "$\delta$"$=0.23\Delta=0.23\hat{C}^{1/2}\hat{U}/\sigma$.

In Table 2, it is found that the overall agreement is satisfactory but the theoretical values of the phase θ are somewhat larger than the experimental estimates. It may be remarked that Jonsson's semi-empirical formula for the friction factor reads, in terms of the notations

Table 2. Comparison of experiments (Jonsson 1963, Carlsen, 1967) with theoretical prediction.

	$\hat{U}/(\sigma z_0)$	Friction Factor $2\hat{C}\cdot10^2$	Phase θ	Energy Loss $<E>/\rho\cdot 10^{-4}$ cm^3/sec^3	Boundary Layer Thickness "δ" cm
Test No. 1 (Jonsson, 1963)	3.66×10^3	2.00	25°	3.92	6.00
Theory		1.82	29°	3.74	6.25
Test No. 2 (Carlsen, 1967)	8.52×10^2	3.95	30°	2.88	5.70
Theory		3.76	43°	2.31	5.64

in the present paper,

$$\frac{0.41}{\sqrt{\hat{C}}}+\ln\frac{1}{\sqrt{\hat{C}}}=-1.852+\ln\left(\frac{\hat{U}}{\sigma z_0}\right). \tag{6-3}$$

On the other hand, (4-45) becomes, by substitution of relevant numerical values,

$$\frac{0.4}{\sqrt{\hat{C}}}+\ln\frac{1}{\sqrt{\hat{C}}}=-2.25+\ln\left(\frac{\hat{U}}{\sigma z_0}\right). \tag{6-4}$$

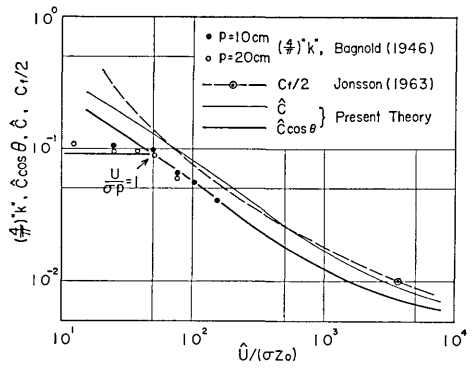

Fig. 9. Comparison of the theoretical prediction of the friction coefficient with Bagnold's data and Jonsson's empirical formula.

The difference between (6-3) and (6-4) is roughly about 10 percent in the friction coefficient. Fig. 9 shows the comparison of the friction coefficients by Bagnold and Jonsson with the prediction based on the present model.

iii) Yalin and Russel (1966) measured bottom shear stresses due to long waves and proposed a formula

$$\tau_B/\rho=\alpha\,|\,u\,|\,u+\beta gsH, \tag{6-5}$$

where α and β are experimental constant, u is the velocity measured at a point 4.5 cm ($\sim H/4$) below the mean water level in a channel of depth $H(=8.5\,\text{cm})$, s is the surface slope and g is the acceleration due to gravity. The experimental ranges of periods T and wave heights $H_{\max}$ are: $2\,\text{min.}<T<20\,\text{min.}$, $0.5\,\text{cm}<H_{\max}<2.5\,\text{cm}$ and two kinds of equivalent roughness D(5 mm and 3 mm) are used. If we make use of the potential theory of waves, the experimental range was approximately given by $6<\hat{U}/(\sigma H)<147$. Referring to the discussion in §2, in this experimental range of $\hat{U}/(\sigma H)$, the depth H plays an increasingly important role with increasing $\hat{U}/(\sigma H)$, so that it is better to compare the experimental result with theoretical prediction given in Paper [1]. If we assume u in the experiment is the mean velocity $\bar{u}$ in Paper [1], and approximate gs by $(i\sigma\bar{u})$, which is a good approximation, at least when the thickness of the frictional layer is thin compared with the total

depth[3], (6-5) may be transformed to

$$\tau_B/\rho=\alpha\left(1+i\frac{\beta}{\alpha}\frac{\sigma H}{\tilde{u}}\right)\tilde{u}\overline{u}, \tag{6-6}$$

where $|u|u$ is approximated by $\tilde{u}\overline{u}$ with $\tilde{u}=\frac{8}{3\pi}\hat{u}$. Therefore, the friction coefficient $C^{(1)}$ defined in Paper [1], (3-23) becomes

$$C^{(1)}=\alpha\sqrt{1+\left(\frac{\beta}{\alpha}\frac{\sigma H}{\tilde{u}}\right)^2}, \tag{6-7a}$$

$$\tan\theta=\frac{\beta}{\alpha}\left(\frac{\sigma H}{\tilde{u}}\right). \tag{6-7b}$$

Yalin and Russel put

$$\alpha=4.41\times10^{-3},\quad \beta=1.8\times10^{-2},\ \text{for } H/D=37, \tag{6-8a}$$

$$\alpha=3.75\times10^{-3},\quad \beta=1.8\times10^{-2},\ \text{for } H/D=61.7, \tag{6-8b}$$

and mentioned that the differences of α, β for the two relative depths were difficult to identify because of the scatter of data points. The values of $C^{(1)}$ and θ, computed from (6-7a, b) with the above numerical values may be compared with the theoretical prediction given in Paper [1]- Fig. 2a, b, for the experimental range $5<\tilde{u}/(\sigma H)<130$ (in Paper [1], the water depth is written as z_h instead of H). For small values of $\tilde{u}/(\sigma H)$, we can use Fig. 7a, b of the present paper, which give the revised version of the friction coefficient of Paper [1] for the deep water condition. Taking the relations $C^{(1)}=\frac{3\pi}{8}C$ and $\frac{\tilde{u}}{\sigma H}=\left(\frac{8}{3\pi}\right)\cdot\frac{1}{30}\cdot\frac{D}{H}\cdot\frac{\hat{U}}{\sigma z_0}$ into account, we may find $\hat{C}^{(1)}$ and θ from Fig. 7a, b.

Sample estimates of the friction coefficients are given in Table 3, in which we see that the phases of the friction coefficient are reasonably close, but that the theoretical predictions of $\hat{C}^{(1)}$ are consistently higher than the empirical estimates by (6-7a) This is the opposite trend to the case given in Table 2. However, taking the uncertainty of the replacement of (6-5) by (6-6) and the determination of α and β into consideration, we may say that the overall agreement is fairly good. For $\tilde{u}/(\sigma H)\gtrsim10^2$,

3) For small values of $\hat{U}/(\sigma H)$, $\overline{u}\sim U$. For large values of $\hat{U}/(\sigma H)$, say, for $\hat{\overline{u}}/(\sigma H)=10^2$, $\hat{\overline{u}}/\hat{U}\sim0.9\ \mathrm{expi}(0.45)$ from Fig. 4a, b of Paper [1], and it may be better to approximate gs by $i\sigma\hat{U}$. At any rate in this situation, βgsH is negligible compared with $\alpha|u|u$.

Table 3. Comparison of the estimates of the friction coefficient derived from the theory and experiment.

H/D	$\tilde{u}/(\sigma H)$	$\hat{U}/(\sigma z_0)$	Theory, Paper [1]		Theory Present Paper		Empirical Formula Eqs. (6-7a, b)	
			$\hat{C}^{(1)}\cdot 10^3$	θ	$\hat{C}^{(1)}\cdot 10^3$	θ	$\hat{C}^{(1)}\cdot 10^3$	θ
37	10^2		5.3	0.040	—	—	4.41	0.041
61.7			4.6	0.040	—	—	3.75	0.048
37	10	1.30×10^4	(7.0)	(0.243)	7.16	0.475	4.74	0.387
61.7		2.18×10^4	(6.0)	(0.240)	6.07	0.435	4.15	0.448

the friction coefficient becomes constant, as shown in Fig. 2a of Paper [1], and in agreement with one of the conclusion given by Yalin and Russel. However, for small values of $\tilde{u}/(\sigma H)$, (6-5) becomes inadequate for the expression of the bottom stresses. Their statement that for small values of T the second term of the expression (6-5) is important, is misleading, because α and β defined by (6-5) can no longer be expected to be constant for small values of $\tilde{u}/(\sigma H)$.

(b) VELOCITY PROFILE

i) As already mentioned in the preceding sub-section, Jonsson (1963) measured the velocity distribution in a turbulent oscillatory flow. However, the oscillatory motions in the experiment were not perfectly sinusoidal due to various experimental limitations, so that his velocity data are subjected to harmonic analysis and velocity amplitudes and phases for the fundamental mode are extracted. The contribution of the higher mode oscillations is found to be about 10 percent of the fundamental mode at each level and seems to show some regularity in the vertical direction, but in the present analysis, only the fundamental mode oscillation is examined.

The experimental conditions for the fundamental mode oscillations are somewhat different from Jonsson's original estimates and it is found that

$$\hat{U}=213.1\ \text{cm/sec},\quad z_0=0.05\ \text{cm},\quad \hat{U}/(\sigma z_0)=5.69\times 10^3, \tag{6-9}$$

where $\hat{U}$ is the mean value of velocity amplitude at three higher levels (height above the crest of a roughness element: 23 cm, 20 cm, 17 cm) and z_0 is estimated by the profile analysis of the velocity amplitude. For the condition (6-9), the friction coefficient is

$$\hat{C}=0.78\times10^{-2},\quad \theta=0.555. \tag{6-10}$$

Now, we compare the observed velocity profile of the fundamental mode with the theoretical one, which is based on (5-3a, b) and can be expressed, with the aid of (5-6), in the form

$$\frac{U-u}{U}=\begin{cases} T(y_R, y)/T(y_R, 0) \text{ for } 0\leq y\leq y_R, & \text{(6-11a)} \\ (2/k)G(y_R)F_2(y)\hat{C}^{1/2}e^{i\theta}, \text{ for } y_R\leq y. & \text{(6-11b)} \end{cases}$$

If we abbreviate (6-11a, b) by

$$(U-u)/U=f_1e^{-if_2}, \tag{6-12}$$

it follows

$$\text{Amp}\,[u/U]=\sqrt{1+f_1^2-2f_1\cos f_2}, \tag{6-13a}$$

$$\text{Phase}\,[u/U]=\tan^{-1}[f_1\sin f_2/(1-f_1\cos f_2)]. \tag{6-13b}$$

Therefore, the theoretical values of amplitudes and phases of u/U as a function of z can be computed readily. Namely, for the condition (6-9) and (6-10), we have

$$\begin{aligned} &\hat{u}_B^*=18.22,\quad y^2=0.3979z,\quad d=1.231\text{ cm} \\ &y_R=0.5463,\quad \hat{G}(y_R)=1.563,\quad \psi=-1.594. \end{aligned} \tag{6-14}$$

The computed values of amplitudes and phases are shown in Fig. 10a, b together with the experimental values. The zero level of the experiment is adjusted, following Jonsson, to be 0.25 cm below the crest of the roughness element. From the figure, it may be concluded that the overall agreement between theory and experiment is good in both amplitude and phase, suggesting that the estimated roughness length z_0 and the height of the overlap layer d are also reasonable. It is mentioned here that if we increase z_0 from 0.05 cm to 0.077 cm as Jonsson estimated, the velocity profile moves upwards in the figure, and if we assume a larger value of K (or d) the level of the maximum amplitude moves upwards. The discrepancy of the detailed shape of the profiles may indicate the limitation of the present theory and to some extent the deficiency of the experiment in the lowermost levels.

ii) Kalkanis (1964) measured the velocity distribution in a turbulent oscillatory flow induced by the periodic oscillation of a flat plate at the bottom and presented data on the amplitude and phase relative to the movement of the plate, namely, f_1 and f_2 in (6-12). The empirical formulas proposed by Kalkanis seems to indicate that the experiment

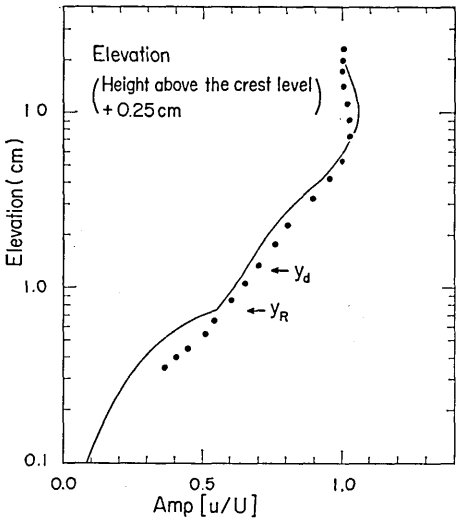

Fig. 10a. Comparison of the theoretical prediction of the amplitude profile of velocity (full line) with Jonsson's 1963 data (black dots). y_d and y_R indicate the upper and lower boundaries of the overlap layer.

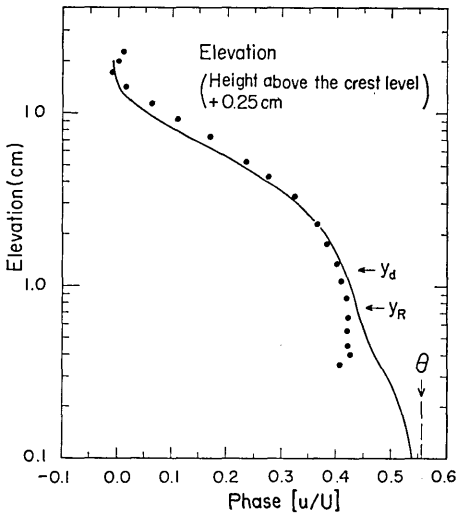

Fig. 10b. Comparison of the theoretical prediction of the profile of phases (full line) with Jonsson's 1963 data (black dots). y_d and y_R indicate the upper and lower boundaries of the overlap layer and θ is the theoretical phase angle between the outer velocity U and the bottom stress τ_B.

may not be in the range of a fully developed turbulence, because the length scale $\delta_L=\sqrt{\nu/\sigma}$ plays a very important role, in contrast to our expectation that the important length scale does not depend on ν for a fully developed turbulence over a rough bottom.

Now let us re-examine the data in the light of the present theory. Since most of his data are found to be in the outer layer, we concentrate our analysis for the outer layer only, where we have from (5-8b) and (6-11b),

$$f_1=\text{Amp}\,[W]\exp[-5.051z/\Delta], \tag{6-15a}$$

$$f_2=5.051z/\Delta+\text{phase}\,[W], \tag{6-15b}$$

where

$$W=4.523\hat{C}^{1/2}\hat{G}\exp-[\psi+\theta+0.7289]. \tag{6-15c}$$

If y_R exceeds y_d, the expression for W becomes, according to (5-5b) and (5-9a),

$$W=my_R\exp\left[\frac{y_R^2(1+i)}{2\sqrt{2}\,y_d}\right]\Big/(\sqrt{K}\,T(y_R)). \tag{6-15d}$$

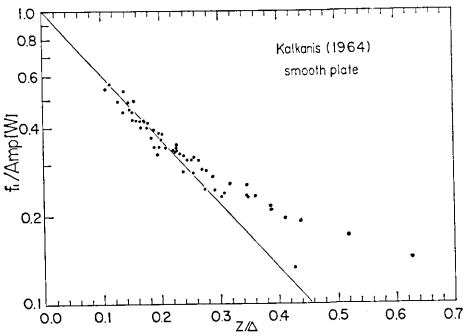

Fig. 11a. Comparison of the theoretical prediction of the amplitude profile of the defect velocity, $f_1/\mathrm{Amp.}[W]$, (full line) with Kalkanis' data for the smooth plate (black dots).

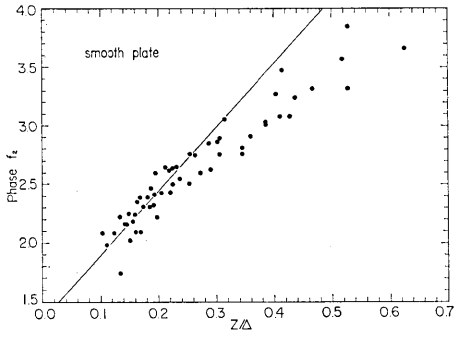

Fig. 11b. Comparison of the theoretical prediction of the phase f_2 with Kalkanis' data for the smooth plate (black dots).

$\hat{C}$, θ, $\hat{G}$, ϕ, Δ, and y_R can be determined from given experimental conditions, if the roughness length z_0 is estimated from the actual roughness.

For the three dimensional roughness $h^{(3)}$ of grains, it is reasonable to assume $z_0=h^{(3)}/30$, but, for the two-dimensional roughness $h^{(2)}$, there is uncertainty about the estimation of z_0. Furthermore, there is a problem of the zero-plane adjustment. Therefore, we omitted the data for the two-dimensional roughness and examined data for the smooth bottom and for the three dimensional roughness with the zero plane adjustment of $0.7\,h^{(3)}$ below the crest level (Kalkanis assumed an adjustment of $0.2\,h^{(3)}$). It is mentioned here, that Jonsson (1966) made a somewhat analogous analysis of Kalkanis' data for the two-dimensional roughness.

For the case of a smooth bottom, the normalized amplitude factor $f_1/\mathrm{Amp}[W]$ and the phase f_2 are shown in Fig. 11a, b respectively, as a function of z/Δ, where the origin of z is displaced 0.06 cm (2×10^{-3} ft.) below the actual bottom to obtain better agreement between the data and the prediction. The theoretical line for $f_1/\mathrm{Amp}[W]$ can be easily drawn by using (6-15a). The theoretical line for f_2 given by (6-15b) is a linear function of z/Δ with the constant factor Phase $[W]$ at $z/\Delta=0$. In the experimental range of Kalkanis, the values of Phase $[W]$ turn out to be about 0.5 but in Fig. 11b, the constant factor is assumed to be 1.35 instead of 0.5.

Now, in Fig. 11a, it is seen that the experimental values for $z/\Delta\lesssim0.2$ are in agreement with the theoretical line. However, for larger values

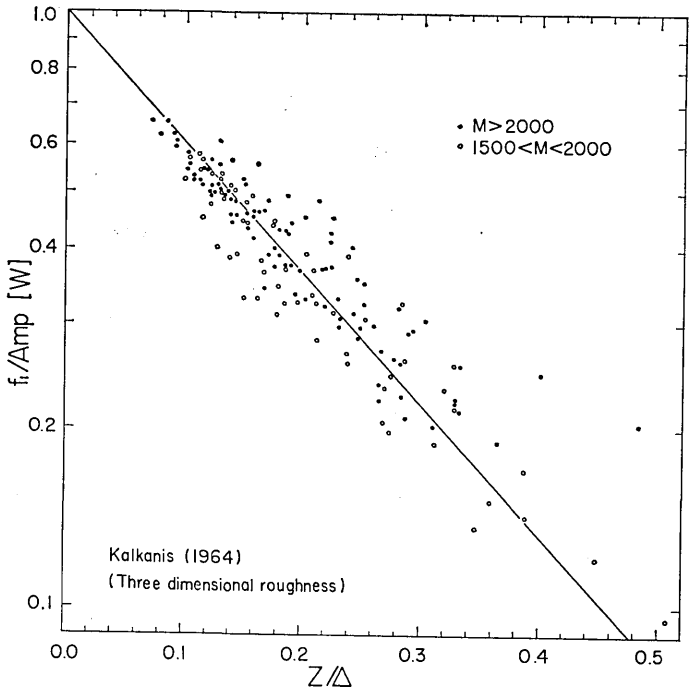

Fig. 12a. Comparison of the theoretical prediction of the defect velocity, $f_1/Amp[W]$, (full line) with Kalkanis' data for the three dimensional roughness on the bottom. Black dots for $M>2000$, and circles for $1500<M<2000$.

of z/Δ, the decrease of the experimental values with height is slower than the theoretical expectation, suggesting the increase of the eddy viscosity with height. Similar tendency can be observed in Fig. 11b where the increase of f_2 with height becomes smaller than the theoretical expectation for $z/\Delta>0.2$. Furthermore, in view of the necessity to make the adjustment in both the zero plane level and the initial phase angle, some factors not included in the present model seem to exist in the inner layer for the case of a smooth bottom.

For the three dimensional roughness, the data are divided into two groups with $M>1500$ and $M<1500$, since, for smaller values of M, the fully developed turbulence may not be realized as discussed in § 4(c). In Fig. 12a, b and Fig. 13a, b the amplitude factor $f_1/$ Amp $[W]$ and the phase f_2 for $M\gtrless1500$ are shown, respectively, together with the theoretical lines. The theoretical line for f_2 is drawn with the initial phase angle of 0.25 which is the average value of Phase $[W]$ in the experimental range.

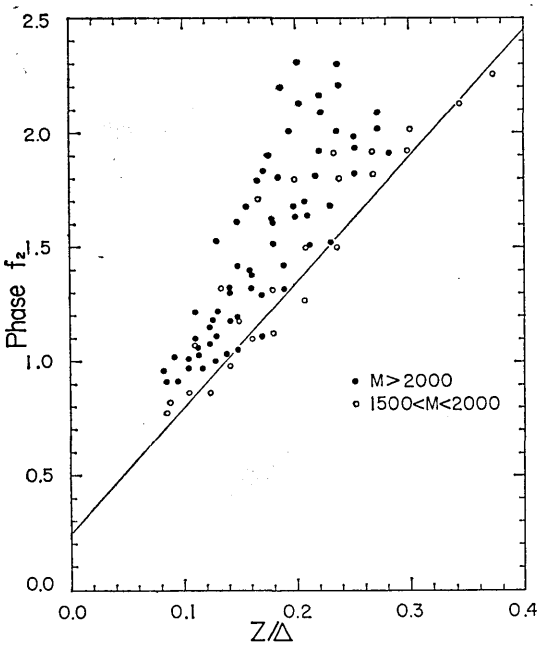

Fig. 12b. Comparison of the theoretical prediction of the phase f_2 with Kalkanis' data for the three dimensional roughness on the bottom. Black dots for $M>2000$, and circles for $1500<M<2000$.

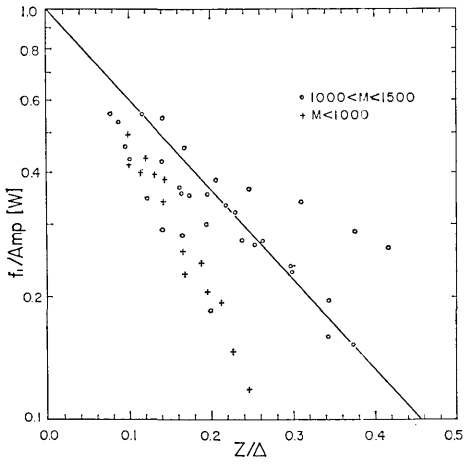

Fig. 13a. Comparison of the theoretical prediction of the defect velocity, $f_1/\mathrm{Amp}\,[W]$, (full line) with Kalkanis' data for the three dimensional roughness on the bottom. Circles for $1000<M<1500$, and crosses for $M<1000$.

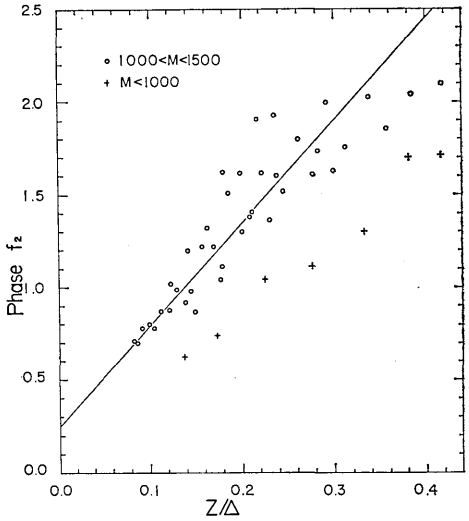

Fig. 13b. Comparison of the theoretical prediction of the phase f_2 with Kalkanis' data for the three dimensional roughness on the bottom. Circles for $1000<M<1500$ and crosses for $M<1000$.

For $M>1500$, the experimental values of $f_1/\mathrm{Amp}[W]$ are in reasonable agreement with the theoretical expectation as seen in Fig. 12a, but the phase f_2 (Fig. 12b) indicates more rapid increase with height than the theoretical values and still shows some dependence on M. For $M<1500$, the experimental values of the amplitude factor scatter in a wide range as shown in Fig. 13a, and show very rapid decrease with height for $M<1000$, suggesting that the fully developed turbulence may not be established. The corresponding phase f_2 for $M<1000$ indicates a very slow increase with height as shown in Fig. 13b.

Judging from Fig. 12a, b and 13a, b, the fully developed turbulence in the outer layer for a moving plate experiment seems to be established for $M>2000$, but the increases of the phase is somewhat faster than the theoretical expectation. For $M<1000$, it seems that the turbulence in the outer layer is distinctly different from the fully developed case and cannot be explained by the present model. It is remarked that the empirical formulas for f_2 given by Kalkanis seems to give better agreement with data than the present prediction.

(c) ONSET OF SAND MOVEMENT UNDER WAVE ACTION

The bottom frictional stress and the movement of sand grains on the bottom of water are expected to be closely related. Following the concept of the critical tractive force producing sand movement in a steady channel flow, we may consider the following relation to hold for the onset of grain movement under wave action:

$$\hat{\tau}_B/(\rho g^* D \tan\varphi)=I, \tag{6-16}$$

where $g^*=g(\rho'-\rho)/\rho$, g is the acceleration due to gravity, ρ and ρ' are the density of water and grain, respectively, D is the grain diameter, and φ is the angle of repose. The complicated relations between forces acting on an individual grain and the mean bottom shear stress are absorbed in the factor I. Although it is essential to clarify the role of I for the understanding of the mechanics of grain movements, we discuss the problem only from the phenomenological point of view. For the case of a steady channel flow, I seems to be a function of u_*D/ν and, for the fully developed turbulence (large values of u_*D/ν), I is practically constant at about 0.05. Near the transition between the hydrodynamically smooth and rough bottom, namely near $u_*D/\nu\sim12$, I reaches a minimum of about 0.03 and below this Reynolds number, I gradually increases up to about 0.15. (See, for example, Ishihara (Ed.), Applied Hydraulics,

II(1), p. 18, Fig. 2.1.12, 1957). Therefore, it is probable that I becomes a constant of the order 0.05 for a turbulent oscillatory flow over a rough bottom.

Now (6-16) is transformed into

$$g^*D/\hat{U}^2=\hat{C}/I, \tag{6-17}$$

and, for a rough turbulent flow, $\hat{C}$ is given as a function of $\hat{U}/(\sigma z_0)$ as shown in Fig. 7a. If we approximate C in the range $3\times10^2<\hat{U}/(\sigma z_0)<10^4$ by

$$\hat{C}=0.6(\sigma z_0/\hat{U})^{1/2}, \tag{6-18}$$

and substitute into (6-17), assuming $D=30z_0$, we have

$$g^*D/\hat{U}^2=\left(\frac{0.11}{I}\right)\left(\frac{\hat{U}}{\sigma D}\right)^{-1/2}. \tag{6-19}$$

An empirical formula given by Bagnold (1946, Eq. 4a) for the initial movement of sand grains is of the form

$$\sigma=A(\hat{U}/\sigma)^{-3/4}g^{*1/2}D^{1/4}, \tag{6-20a}$$

with

$$A=21.5D^{0.075}g^{-0.5}, \quad (C.G.S.\ \text{units}).$$

This formula can be transformed to

$$g^*D/\hat{U}^2=\frac{1}{A^2}\left(\frac{\hat{U}}{\sigma D}\right)^{-1/2}. \tag{6-20b}$$

where the value of A^2 in his experimental range ($0.33\ \text{cm}\leq D<0.09\ \text{cm}$) is $0.417<A^2<0.232$. Therefore, the expected value of I in (6-19) becomes $0.026<I<0.046$ for the initial movement of grains. A similar empirical formula was presented by Sato and Tanaka (1962) for the general movement of grains. Their formula can be reduced to the form (6-19) where $I/0.11=0.6$, so that I becomes 0.066.

For the general movement of grains, more direct comparison between the experimental data and the theory is made by using the data by Manohar (1955), Goddét (1960), Sato and Tanaka (1962), Horikawa and Watanabe (1966).

As discussed in §5-(c), the lower limit of the rough turbulent flow may be delineated by $M>60$ for $R<10^2$, and a little larger value of M for $R>10^2$. However, for simplicity of the discussion, we assumed $M=60$ as the criterion of smooth-rough transition in the whole range

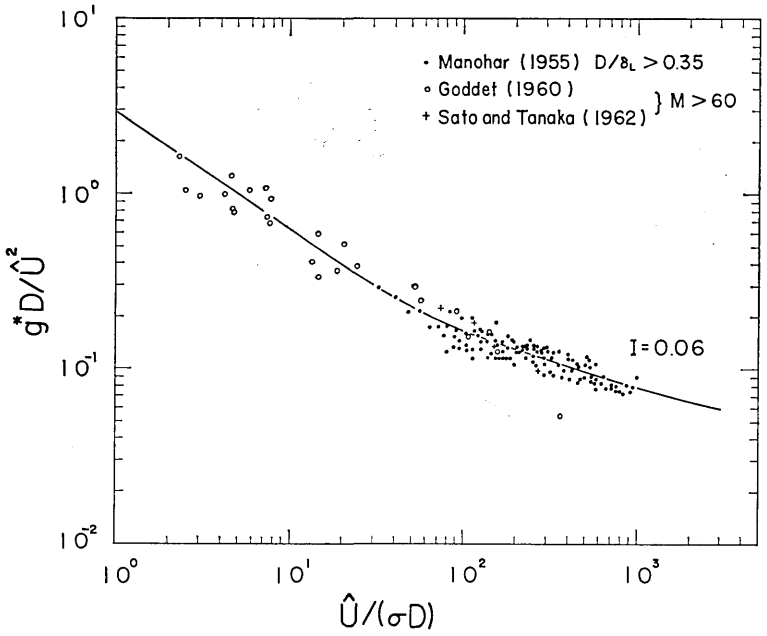

Fig. 14a. Comparison of the theoretical prediction of the general movements of grains (I=0.06) for the rough turbulent flow with experimental data by Manohar (1955), Goddét (1960) and Sato & Tanaka (1962). Criterion of the rough turbulent flow is described in the figure.

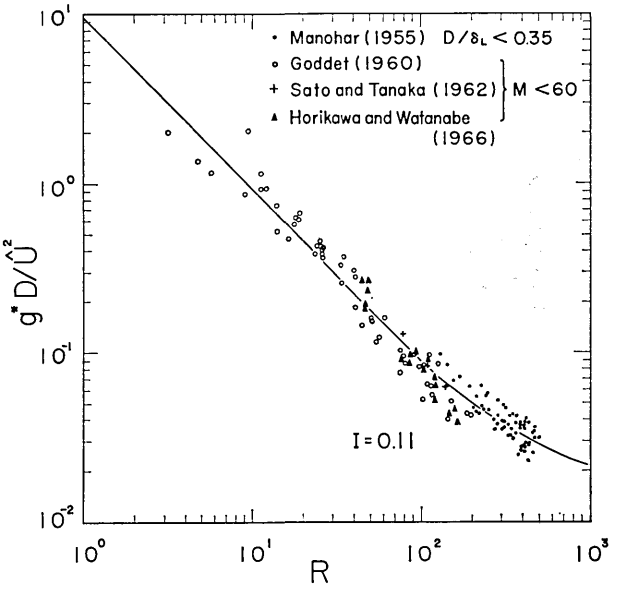

Fig. 14b. Comparison of the theoretical prediction of the general movements of grains (I=0.11) for the laminar or smooth turbulent flow with experimental data by Manohar (1955), Goddét (1960), Sato & Tanaka (1962), and Horikawa & Watanabe (1966). Criterion of the laminar or smooth turbulent flow is described in the figure.

of the experiments by Goddét, Sato and Tanaka, Horikawa and Watanabe. For the data of Manohar, we followed the criterion given by Manohar that $D/\delta_L=0.35$ is the critical value of the smooth-rough transition. In terms of M, therefore, the data by Manohar for $M<120$ are included in the case of a smooth bottom.

In Fig. 14a, the data for a rough turbulent flow are shown as a function of $\hat{U}/(\sigma D)$ with the theoretical curve transcribed from Fig. 7a, assuming $D=30z_0$ and $I=0.06$. In Fig. 14b, the data for a smooth bottom are shown as a function of R with the theoretical curve transcribed from Fig. 6a, assuming $I=0.11$.

As seen in Fig. 14a, b, the experimental results seem to be in fairly good agreement with the theoretical prediction with $I=0.06$ for a rough turbulent flow and $I=0.11$ for a smooth flow. This, in turn, means that the theoretical prediction of the friction coefficient may be realistic. It is remarked here that the data of Goddét for $M<60$ and $R<10^2$ do not show any systematic deviation from the data for $M>60$ if plotted in Fig. 14a for a rough bottom. This suggests the difficulty of separating the smooth and rough bottom for small values of M and R. Horikawa *et al.* (1966) made a similar analysis for the initial and general movements of grains on the basis of the result given in Paper [1]. However, since the friction formula given in Paper [1] was not adequate for small values of $\hat{U}/(\sigma z_0)$, their conclusions should be revised accordingly.

7. Summary and conclusion

The eddy viscosity assumptions [(3-2a, b, c), (3-6a, b)] analogous to those for the steady flow in a turbulent boundary layer are introduced by defining various quantities in the oscillatory flow, such as the modified friction velocity u^*[(2-16)], the wave displacement thickness δ^*[(2-17)], and the vertical scale of the defect layer Δ[(2-18)]. The boundary layer is divided into three parts: inner, overlap, and outer layer, and two universal constants $k(=0.4)$ and $K(=0.02)$ are assumed. In particular, the effective viscosity in the inner layer is assumed somewhat differently from that commonly used for the steady flow and we introduce a constant Reynolds number $N(=12)$ related to the viscous sub-layer and the roughness height $D_R(=15z_0)$ (§ 3).

Making use of the eddy viscosity assumptions, the linearized equation of oscillatory motions in the boundary layer is solved for the case of a boundary layer thin compared with the total depth of water. The

vertical distributions of shear stress and velocity, and also the friction coefficient can be derived straightforwardly (§ 5). In particular, in the defect layer, the shear stress and defect velocity can be expressed in universal forms, F_1 and F_2 (Fig. 3a, b), if they are suitably nondimensionalized by means of Gu_B^* and Δ. The parameter G and the friction coefficient C, both of which are defined in complex forms, are functions of $R(=\hat{U}\delta_L/\nu)$ or $\hat{U}/(\sigma z_0)$ only and are shown in Fig. 2, Fig. 6a, b, Fig. 7a, b.

The comparison of the present theory with empirical results shows reasonable agreement in both the velocity profile and the friction coefficient (or energy dissipation). The critical tractive force for the movement of sand grains under wave action can also be formulated parallel to the case of steady turbulent flow, by making use of the present formula of the friction coefficient (§ 6).

The gross features of the boundary layer under waves are thus simulated satisfactorily. However, if we look into the details of the structure of boundary layer, it is obvious that the discussion based on a model assuming the average state of turbulence over one wave period cannot be sufficient. The instantaneous state of turbulence is completely left out of the consideration, and we are not certain how the instantaneous state of turbulence and the average state of turbulence as assumed in the present paper can be related. For the development of the study of a wave boundary layer, it seems essential, at first, to understand the generation and maintenance of turbulence on a more rigorous basis.

As for the rough surface, our knowledge is far from satisfactory. Among many problems related to the rough surface, we need more definite knowledge about the roughness length z_0 or its equivalent, and the location of the zero plane, in view of the fact that for small values of $\hat{U}/(\sigma z_0)$, the scale of the boundary layer δ^* becomes comparable to the height of roughness elements.

Reference

BAGNOLD, R. A., 1946, Motion of wave in shallow water; Interaction between waves and sand bottoms, *Proc. Roy. Soc. London A*, **187**, 1-18.

BRETSCHNEIDER, C. L., 1954, Field investigation of wave energy loss of shallow water ocean waves, *Beach Erosion Board, Tech. Memo.* No. 46, 1-21.

CARLSEN, N. A., 1967, Measurement in the turbulent wave boundary layer, *Basic Res., Progress Rep.* No. 14, Coastal Engineering Lab., Tech. Univ. of Denmark.

CLAUSER, F. H., 1956, The turbulent boundary layer, *Advances in Applied Mechanics,*

4, 1-51, Academic Press, New York.

COLEBROOK, C. F., and C. M. WHITE, 1937, Experiments with fluid friction in roughened pipes, *Proc. Roy. Soc. London A*, **161**, 367-381.

COLLINS, J. I., 1963, Inception of turbulence at the bed under periodic gravity waves, *J. Geophys. Res.*, **68**, 6007-6014.

GODDÉT, J., 1960, Etude du début d'entrainment des matériaux mobiles sous l'action de la houle, *La Houille Blanche*, No. 2, 122-135.

HORIKAWA, K. and F. WATANABE, 1966, A consideration on sand movement under wave action, *Proc. 13th Conf. Coastal Engineering in Japan*, 126-134 (in Japanese).

INMAN, D. L., 1962, Flume experiments on sand transport by waves and currents, *Proc. 8th Conf. Coastal Engineering, Mexico City*, 137-150.

ISHIHARA (Editor), 1957, *Applied Hydraulics*, **II** (**1**), Maruzen Co., Tokyo, (in Japanese).

IWAGAKI, Y., and T. KAKINUMA, 1964, Some observations on the modification of wind waves and swells in shallow water, *Proc. 11th Conf. Coastal Engineering in Japan*, 49-55, (in Japanese).

IWAGAKI, Y., Y. TSUCHIYA, and H. CHEN, 1967, On the mechanism of laminar damping of oscillatory waves due to bottom friction, *Bull. Disas. Prev. Res. Inst., Kyoto Univ.*, **16** (3), No. 116, 49-75.

JONSSON, I. G., 1963, Measurements in the turbulent wave boundary layer, *10th Congress*, I. A. H. R., London, **1**, 85-92.

JONSSON, I. G., 1966, On the existence of universal velocity distributions in an oscillatory, turbulent boundary layer, *Basic Res. Progress Rep.* No. 12, Coastal Engineering Lab., Tech. Univ. of Denmark.

JONSSON, I. G., 1967, Wave bundary layers and friction factors, *Proc. 10th Conf. Coastal Engineering, Tokyo*, 127-148.

KAJIURA, K., 1964, On the bottom friction in an oscillatory current, *Bull. Earthq. Res. Inst.*, **42**, 147-174.

KALKANIS, G., 1964, Transportation of bed material due to wave action, *U.S. Army Coastal Engineering Research Center, Tech. Memo.* No. 2.

LI, H., 1954, Stability of oscillatory laminar flow along a wall, *Beach Erosion Board, Tech. Memo.* No. 47.

LUKASIK, S. J., and C. E. GROSCH, 1963, Pressure-velocity correlations in ocean swells, *J. Geophys. Res.*, **68**, 5689-5699.

MANOHAR, M., 1955, Mechanics of bottom sediment due to wave action, *Beach Erosion Board, Tech. Memo.* No. 75.

MELLOR, G. L., and D. M. GIBSON, 1966, Equilibrium tubulent boundary layers, *J. Fluid Mech.*, **24**, 225-253.

MELLOR, G. L., 1966, The effects of pressure gradients on turbulent flow near a smooth wall, *J. Fluid Mech.*, **24**, 255-274.

MOTZFELD, H., 1937, Die turbulente Strömung an welligen Wanden, *Z. angew. Math. u, Mech.*, **17**, 193-212.

PUTNAM, J. A., and J. W. JOHNSON, 1949, The dissipation of wave energy by bottom friction, *Trans. Amer. Geophys. Union*, **30**, 67-74.

ROUSE, H., 1937, Modern conceptions of the mechanics of fluid turbulence, *Trans. Amer. Soc. Civil Engrs.*, **102**, 463-543.

SATO, S., and N. TANAKA, 1962, On the sand movement on a horizontal bed due to wave action, *Proc. 9th Conf. Coastal Engineering in Japan*, 95-100, (in Japanese).

SAVAGE, R. P., 1953, Laboratory study of wave energy losses by bottom friction and

percolation, *Beach Erosion Board, Tech. Memo.* No. 31.
VINCENT, G. E., 1957, Contribution to the study of sediment transport on a horizontal bed due to wave action, *Proc. 6th Conf. Coastal Engineering, Florida*, 326-335.
YALIN, M. S., and R. C. H. RUSSEL, 1966, Shear stresses due to long waves, *J. Hydr. Res.*, **4** (2), 56-98.
ZHUKOVETS, A. M., 1963, The influence of bottom roughness on wave motion in a shallow body of water, *Bull. Acad. Sci., USSR, Geophys. Ser.*, No. 10, 1561-1570, Transl. 943-948.

---

5. 波に伴なう水底摩擦境界層について

地震研究所 梶 浦 欣 二 郎

水粒子の周期運動によって水底に生ずる乱流境界層に関して，前論文（梶浦，1964）では，摩擦層が水面に及ぶ様な周期の長い波の場合を主として取扱ったが，ここでは境界層厚が水深にくらべて小さい場合を考える．

まず，流速 u，境界層外流速 U，摩擦応力 τ，水の密度 ρ から，摩擦速度 u^* ($\tau/\rho=\hat{u}^*u^*$)，排除厚 δ^* ($\delta^*=Amp\int_0^\infty(U-u)dz/\hat{U}$) 等を定義する．ここで，角速度 σ で変化する量は複素数であらわし，振幅には ∧ をつける．(§2)

次に，定常流の場合にならって，境界層を3層に分け，それぞれに対応する定数 $N(=12)$，$k(=0.4)$，$K(=0.02)$ を導入して有効粘性係数 Kz を次の様に仮定する．

$$Kz=\begin{cases}\nu, & 0\leq z<D_L, \quad (\text{内 層}), & (1\text{-a})\\ k\hat{u}_B^*z, & D_L<z\leq d, \quad (\text{中間層}), & (1\text{-b})\\ K\hat{U}\delta^*, & d\leq z, \quad (\text{外 層}), & (1\text{-c})\end{cases}$$

ここで，ν は分子動粘性係数，$\hat{u}_B^*$ は底面摩擦速度の振幅，z は水面からの高さ，D_L は層流底層の厚さ ($\hat{u}_B^*D_L/\nu=N$) であり，中間層の上限の高さ d は，$k\hat{u}_B^*d=K\hat{U}\delta^*$ からきめる．

底面が粗な場合には，内層 (1-a) の代りに，

$$K_z=\alpha k\hat{u}_B^*D_R, \qquad 0\leq z<D_R \qquad (1\text{-d})$$

とおき，z_0 (Nikuradse の相当粗度 $D=30z_0$) を粗度長さとすると，$D_R=15z_0$，$1/\alpha=\ln(D_R/z_0)$ と仮定する．(§3)

境界層内の運動方程式は

$$\frac{\partial}{\partial t}(U-u)=-\frac{\partial}{\partial z}(\tau/\rho), \qquad (2)$$

と近似出来るから，K_z を利用すると (2) を解いて流れの様子は完全にきめられる．(§4)

高さの尺度 $\Delta(\Delta=Amp\int_0^\infty(U-u)dz/\hat{u}_B^*)$ を利用すると，中間層，外層での規格化された速度欠損 $(U-u)$，及び応力 (u^*) の分布は (z/Δ) のみの函数として表示出来る．また，複素摩擦係数 C を $\tau_B/\rho=C\hat{U}U$ で定義すると，その振幅 $\hat{C}$ 及び位相 θ は水底が滑面か粗面かによって，それぞれ $R(=\hat{U}\delta_L/\nu,\ \delta_L=\sqrt{\nu/\sigma})$ 又は $\hat{U}/(\sigma z_0)$ の函数として計算出来るし，単位時間，単位面積あたりの底面摩擦による平均エネルギー消耗率 $\langle E\rangle$ は，

$$\langle E\rangle=(\rho/2)\hat{C}\hat{U}^3\cos\theta, \qquad (3)$$

であらわせる．特に前論文との相違は R 又は $\hat{U}/(\sigma z_0)$ の小さいところであらわれ，滑面の場合には $R\lesssim 100$ で $C\sim e^{i\pi/4}/R$，粗面の場合には $U/(\sigma z_0)\lesssim 700$ で $C\sim(15\alpha k)^{2/3}\left(\frac{\hat{U}}{\sigma z_0}\right)^{-2/3}e^{i\pi/4}$ とな

る.

粗面—滑面の遷移領域を定常流の場合にならって $0.4 \leqq D/D_L \leqq 5$ と考えるとすれば，層流—乱流の遷移領域は，$0.4 \leqq \delta^*/D_L \leqq 5$ と考えるのが適当と思われ，滑面についての Collins (1963) の実験値は $\delta^*/D_L = 0.85$ である．(§ 5)

理論流速分布は Jonsson (1963) の実験値と振幅，位相ともにかなりよい一致を示し，摩擦係数は Bagnold (1946) の実験値を説明し，また波による底面砂の移動限界についても満足すべき説明を与える．(§ 6)